Advanced Calibration for Device Simulation User Guide

Version H-2013.03, March 2013

SYNOPSYS®

Copyright and Proprietary Information Notice

Copyright © 2013 Synopsys, Inc. All rights reserved. This software and documentation contain confidential and proprietary information that is the property of Synopsys, Inc. The software and documentation are furnished under a license agreement and may be used or copied only in accordance with the terms of the license agreement. No part of the software and documentation may be reproduced, transmitted, or translated, in any form or by any means, electronic, mechanical, manual, optical, or otherwise, without prior written permission of Synopsys, Inc., or as expressly provided by the license agreement.

Destination Control Statement

All technical data contained in this publication is subject to the export control laws of the United States of America. Disclosure to nationals of other countries contrary to United States law is prohibited. It is the reader's responsibility to determine the applicable regulations and to comply with them.

Disclaimer

SYNOPSYS, INC., AND ITS LICENSORS MAKE NO WARRANTY OF ANY KIND, EXPRESS OR IMPLIED, WITH REGARD TO THIS MATERIAL, INCLUDING, BUT NOT LIMITED TO, THE IMPLIED WARRANTIES OF MERCHANTABILITY AND FITNESS FOR A PARTICULAR PURPOSE.

Trademarks

Synopsys and certain Synopsys product names are trademarks of Synopsys, as set forth at http://www.synopsys.com/Company/Pages/Trademarks.aspx.
All other product or company names may be trademarks of their respective owners.

Synopsys, Inc.
700 E. Middlefield Road
Mountain View, CA 94043
www.synopsys.com

Contents

About This Guide v

Audience vi
Related Publications vi
Typographic Conventions vi
Customer Support vii
Accessing SolvNet vii
Contacting Synopsys Support vii
Contacting Your Local TCAD Support Team Directly viii

Chapter 1 Using Advanced Calibration File of Sentaurus Device 1

Overview 1
Location of Advanced Calibration File 1
Using Advanced Calibration Device 2

Chapter 2 Content of Advanced Calibration Device 3

Target Devices and Technologies 3

Chapter 3 Guide to Device Simulation 5

Specifying Simulation Cases 5
Access to Parameter Files and Model Frameworks 6
Path A: Basic CMOS Simulation Command File Sections 6
Path B: Adding Influence of Mechanical Stress to Physics Section Shown Under Path A 7
Path C: Adding High-k Mobility Degradation to Physics Section Shown Under Path B 9
Path D: FinFET Simulations – Use Path C 10
Path E: Thin-Layer MOS Simulations – Inclusion of Thin-Film Effects 10
Path F: GaN HEMT Simulations 11
Path G: SiC Diode Simulations 12
References 13

Chapter 4 Guide for Calibration of Device Simulations 15

Calibration Methodology 15
Calibration of Planar CMOS Devices with Silicon Channel 15

CV Calibration . . . 16
Long-Channel Id–Vg Calibration . . . 17
Short-Channel Id–Vg Calibration at Low Drain Bias . . . 19
Short-Channel Id–Vg Calibration at High Drain Bias . . . 21
References . . . 22

Chapter 5 Review of Models **23**

Overview of Models . . . 23
CMOS Devices . . . 23
Unstrained Band Structure and Electrostatics . . . 23
Strained Band Structure and Electrostatics . . . 23
Unstrained Low-Field Mobility . . . 24
Strained Low-Field Mobility . . . 27
Influence of Mechanical Stress . . . 27
Piezoresistance Mobility Models . . . 29
Occupation-based and Band Structure-based Models . . . 31
Unstrained High-Field Mobility . . . 32
Strained High-Field Mobility . . . 33
Gallium Nitride HEMTs . . . 34
Silicon Carbide Devices . . . 34
Silicon Smart-Power and Power Devices . . . 34

Chapter 6 Parameter Files **37**

Content of Parameter Files . . . 37

Chapter 7 Quality of Fitting and Extraction **41**

Low-Field Mobility of Planar CMOS Devices with Silicon Channel and Oxide–Silicon Interface . . . 41
Basic Properties of Silicon Carbide Devices . . . 48
References . . . 53

Appendix A Description of PMI Model MCmob **57**

Overview . . . 57
Parameters . . . 58

About This Guide

Sentaurus Device is a quantum drift-diffusion device simulator for solving the semiconductor equations in one, two, or three spatial dimensions.

Extensions for hydrodynamic transport, solution of the heat conduction equation, and many other features are available as well. Because of the large number of models and the corresponding model parameters and their dependency on fabrication processes and device types, it is difficult to derive automatically a well-adjusted device simulation environment for specific simulation tasks. Therefore, preselection of models and precalibration of parameter sets are necessary. This preselection and precalibration is called Advanced Calibration Device.

This documentation is a user guide for the Advanced Calibration of Sentaurus Device:

- Chapter 1 introduces Advanced Calibration Device.
- Chapter 2 specifies the target devices and technologies for Advanced Calibration Device.
- Chapter 3 guides users from the simulation problem to the selection of parameter sets and device models.
- Chapter 4 introduces calibration methodologies for device simulation.
- Chapter 5 provides a review of models.
- Chapter 6 discusses the parameter files.
- Chapter 7 discusses fitting quality and extraction issues.

Synopsys is working continually on improving the simulation models and optimizing the model parameters for the latest technology nodes. This effort is based on long-standing experience of model calibration for customers and a comprehensive, growing knowledge about device simulation methodologies. The variety of partners and data ensures that systematic and random errors in experimental work are minimized in this model representation.

Advanced Calibration Device provides users with a set of parameters for CMOS technologies from micrometer dimensions down to 28 nm and 16 nm nodes, including planar gate-first and gate-last technologies, nonplanar technologies for the 16 nm node, and technologies beyond 16 nm likely based on novel channel materials (SiGe and Ge). In addition, Advanced Calibration Device delivers parameter sets for GaN HEMTs and SiC devices.

The requirements of device simulation and device calibration approaches are discussed.

This user guide is designed to give fast access to parameter sets and model selections needed for simulation. Therefore, the first chapters provide a guide from the simulation problem to the selection of parameter sets and device models.

Audience

In this guide, the contents, use, and syntax of the Advanced Calibration files for Sentaurus Device are explained. It is directed at users who are familiar with the use of Sentaurus Device and want to obtain a higher accuracy in device simulation.

For detailed information about Sentaurus Device, refer to the *Sentaurus Device User Guide*.

Related Publications

For additional information about Advanced Calibration, see:

- The TCAD Sentaurus release notes, available on SolvNet (see Accessing SolvNet).
- Documentation available through SolvNet at https://solvnet.synopsys.com/DocsOnWeb.

Typographic Conventions

Convention	Explanation
Blue text	Identifies a cross-reference (only on the screen).
Bold text	Identifies a selectable icon, button, menu, or tab. It also indicates the name of a field or an option.
`Courier font`	Identifies text that is displayed on the screen or that the user must type. It identifies the names of files, directories, paths, parameters, keywords, and variables.
Italicized text	Used for emphasis, the titles of books and journals, and non-English words. It also identifies components of an equation or a formula, a placeholder, or an identifier.
Key+Key	Indicates keyboard actions, for example, Ctrl+I (press the I key while pressing the Control key).
Menu > **Command**	Indicates a menu command, for example, **File** > **New** (from the **File** menu, select **New**).
NOTE	Identifies important information.

Customer Support

Customer support is available through SolvNet online customer support and through contacting the Synopsys support center.

Accessing SolvNet

SolvNet includes an electronic knowledge base of technical articles and answers to frequently asked questions about Synopsys tools. SolvNet also gives you access to a wide range of Synopsys online services, which include downloading software, viewing documentation, and entering a call to the Synopsys support center.

To access SolvNet:

1. Go to the SolvNet Web page at https://solvnet.synopsys.com.
2. If prompted, enter your user name and password. (If you do not have a Synopsys user name and password, follow the instructions to register with SolvNet.)

If you need help using SolvNet, click Help on the SolvNet menu bar.

Contacting Synopsys Support

If you have problems, questions, or suggestions, you can contact Synopsys support in the following ways:

- Go to the Synopsys Global Support Centers site on www.synopsys.com. There you can find e-mail addresses and telephone numbers for Synopsys support centers throughout the world.
- Go to either the Synopsys SolvNet site or the Synopsys Global Support Centers site and open a case online (Synopsys user name and password required).

Contacting Your Local TCAD Support Team Directly

Send an e-mail message to:

- support-tcad-us@synopsys.com from within North America and South America.
- support-tcad-eu@synopsys.com from within Europe.
- support-tcad-ap@synopsys.com from within Asia Pacific (China, Taiwan, Singapore, Malaysia, India, Australia).
- support-tcad-kr@synopsys.com from Korea.
- support-tcad-jp@synopsys.com from Japan.

CHAPTER 1 Using Advanced Calibration File of Sentaurus Device

This chapter gives a brief introduction to the use of Advanced Calibration in a device simulation with Sentaurus Device.

Overview

Advanced Calibration Device is a selection of models and parameters that is recommended to be used for device simulation of certain device types and technologies. This selection of models and parameters is contained in text files, which can be opened with any standard text editor.

By starting Sentaurus Device with the corresponding Advanced Calibration Device command file section and loading the Advanced Calibration Device parameter file from that command file, the standard calibration of Synopsys is selected.

For more information about how to use the command file, which defines the models, and the parameter file, which defines the parameters of the models selected in the command file, refer to the *Sentaurus Device User Guide*.

Location of Advanced Calibration File

For each release of Synopsys TCAD, there are new Advanced Calibration Device files that include the latest set of models and parameters. The parameter files are stored in the `MaterialDB` folder of the standard installation of Sentaurus Device. Currently, the files `CMOS.par`, `WBG.par`, `AlN.par`, `AlGaN.par`, `GaN.par`, `4H-SiC.par`, and `6H-SiC.par` are available.

The parameter file and command file sections for the Advanced Calibration of Sentaurus Device are described in this user guide. They represent Version H-2013.03 of Advanced Calibration Device.

Using Advanced Calibration Device

To use the Advanced Calibration of Sentaurus Device, you can look up the parameter files and the command files that are best suited for your device and technology requirements in Chapter 3 on page 5.

CHAPTER 2 Content of Advanced Calibration Device

This chapter specifies the target devices and technologies for Advanced Calibration Device.

Target Devices and Technologies

This version of Advanced Calibration Device focuses on technology nodes starting from several micrometers and going down to 14 nm, based on silicon, germanium, and SiGe channel materials. In addition, parameters and models for smart-power and power devices, GaN HEMTs, and SiC diodes and MOSFETs are provided and discussed.

The main process features of silicon, germanium, and SiGe planar and nonplanar bulk and SOI technology nodes that should be covered by the model and parameter sets are:

- Stress engineering with SiGe pockets (PMOS), SiC pockets (NMOS), single stress liner or dual stress liner, and process-induced stress (metal gate, shallow trench isolation, contact plugs, and so on)
- Poly/SiON or metal/HfO_2/SiON gate stacks
- Gate-first and gate-last technologies
- Silicon, germanium, and SiGe channel

The main device types included are:

- Low-power and high-performance NMOS and PMOS with silicon, germanium, or SiGe channel
- Silicon smart-power and power devices
- GaN HEMTs
- SiC diodes and MOSFETs

For the abovementioned devices and technologies, Advanced Calibration Device provides model selections and parameter sets for the simulation of the following device properties:

- Electrostatic properties and quantization
- Low-field and high-field mobility
- Stress dependency of mobility

NOTE The parameter sets must be considered as inital parameter sets, that is, starting points for further calibration.

CHAPTER 3 Guide to Device Simulation

This chapter provides a guide for the selection of parameter sets and device models.

In this chapter, users can select parameter sets and models quickly. The chapter is organized in the following way: Table 1 and Table 2 present typical simulation cases. In the tables, a path is defined that can be used to select the proper device simulation parameter set and the appropriate `Physics` section for the command file.

Specifying Simulation Cases

In Table 1 and Table 2, the characters A to G indicate different paths that are described in detail in the following sections.

Table 1 Specifying the simulation case: CMOS

Node	**> 130 nm**	**45–130 nm**	**32–45 nm**			**28 nm**				**22 nm**	**< 22 nm**				
Selection path	A	B	B	C	C	B	C	C	C	C	C	D	E	D	D
Planar bulk and SOI	X	X	X	X	X	X	X	X	X	X	X				
FinFET												X		X	X
Thin film													X		
Si	X	X	X	X		X	X		X	X	X	X	X		
SiGe					X			X						X	
Ge															X
Gate-first	X	X	X			X									
Gate-first with metal gate				X	X		X	X							
Gate-last with metal gate									X	X	X	X	X	X	X
Without stress	X														
With stress		X	X	X	X	X	X	X	X	X	X	X	X	X	X

Table 2 Specifying the simulation case: Smart power and power

Node	HVMOS	LDMOS	IGBT	HEMT	Diode
Selection path	A	A	A	F	G
Si	X	X	X		
SiGe					
SiC					X
GaN				X	

Access to Parameter Files and Model Frameworks

The following sections give access to the model frameworks and the parameter files.

Path A: Basic CMOS Simulation Command File Sections

For quantization, the density gradient model of Sentaurus Device is used (`eQuantumPotential` and `hQuantumPotential`).

The orientation of the conducting interface is detected automatically. However, the channel or the current flow direction must be defined manually using the correct mobility parameter set in the parameter file.

```
Files {
   Parameters="$STROOT/tcad/$STRELEASE/lib/sdevice/MaterialDB/CMOS.par"
   ...
}

Physics {
   eQuantumPotential hQuantumPotential
   Mobility (
      -ConstantMobility
      Enormal (
         IALmob(AutoOrientation=1 PhononCombination=1 FullPhuMob=1)
      )
      HighFieldSaturation(EparallelToInterface))
   EffectiveIntrinsicDensity(Slotboom Fermi)
}
```

Path B: Adding Influence of Mechanical Stress to Physics Section Shown Under Path A

Taking into account mechanical stress, the low-field mobility model must be combined with a model describing the stress influence. There are two ways to model the mobility change by mechanical stress:

- First, you can use the `eSubband` and `hSubband` models for a strongly based physical calculation of the mobility enhancement by mechanical stress in silicon devices that is directly based on band structure and subbands. For the subband models, the channel direction must be set in the command file when it is not the <110> channel.
- Second, you can use the `MCmob` model when the subband models are not applicable or calibrated (SiGe or Ge channel material), or when the computation speed is extremely important (complex 3D simulation). For `MCmob`, the channel direction must be set in the parameter file (see Appendix A on page 57).

With subband models:

```
Files {
   Parameters="$STROOT/tcad/$STRELEASE/lib/sdevice/MaterialDB/CMOS.par"
   ...
}

Physics {
   eQuantumPotential hQuantumPotential
   Mobility (
      -ConstantMobility
      Enormal (
         IALmob(AutoOrientation=1 PhononCombination=1 FullPhuMob=1)
      )
      HighFieldSaturation(EparallelToInterface))
   EffectiveIntrinsicDensity(Slotboom Fermi)

   eMultivalley(MLDA kpDOS -density)
   Piezo (
      Model (
         Mobility (
            saturationfactor=0.0
            eSubband(Doping EffectiveMass Scattering(MLDA))
               # eSubband(Doping EffectiveMass Scattering(MLDA) -RelChDir110)
               # for <100> channel
               # hSubband(Doping EffectiveMass Scattering(MLDA))
               # for holes
         )
```

```
         DOS(eMass hMass)
         DeformationPotential(Minimum ekp hkp)
      )
   )
}
```

With the `MCmob` model:

```
Files {
   Parameters="$STROOT/tcad/$STRELEASE/lib/sdevice/MaterialDB/CMOS.par"
   ...
}

Physics {
   eQuantumPotential hQuantumPotential
   Mobility (
      -ConstantMobility
      Enormal (
         IALmob(AutoOrientation=1 PhononCombination=1 FullPhuMob=1)
      )
      HighFieldSaturation(EparallelToInterface))
   EffectiveIntrinsicDensity(Slotboom Fermi)

   Piezo (
      Model (
         Mobility (
            saturationfactor=0.0
            factor(Kanda sfactor=MCmob(Type=0))   # Type=1 for holes
         )
         DOS(eMass hMass)
         DeformationPotential(Minimum ekp hkp)
      )
   )
}
```

The command file section above is designed for electron transport (NMOS). For hole transport (PMOS), you must replace `eSubband` with `hSubband`, and specify `Type=1` for `MCmob`.

Path C: Adding High-k Mobility Degradation to Physics Section Shown Under Path B

```
Files {
   Parameters="$STROOT/tcad/$STRELEASE/lib/sdevice/MaterialDB/CMOS.par"
   ...
}

Physics {
   eQuantumPotential hQuantumPotential
   Mobility (
      -ConstantMobility
      Enormal (
         IALmob(AutoOrientation=1 PhononCombination=1 FullPhuMob=1)
         Lombardi_highk              # Used for remote phonon scattering (RPS)
         NegInterfaceCharge (SurfaceName="s1")
                                     # Used for remote Coulomb scattering (RCS)
                                     # and remote dipole scattering (RDS)
         PosInterfaceCharge (SurfaceName="s1")
                                     # Used for RCS and RDS
      )
      HighFieldSaturation(EparallelToInterface))
   EffectiveIntrinsicDensity(Slotboom Fermi)

   eMultivalley(MLDA kpDOS -density)
   Piezo (
      Model (
         Mobility (
            saturationfactor=0.0
            eSubband(Doping EffectiveMass Scattering(MLDA))
               # eSubband(Doping EffectiveMass Scattering(MLDA) -RelChDir110)
               # for <100> channel
               # hSubband(Doping EffectiveMass Scattering(MLDA))
               # for holes
         )
         DOS(eMass hMass)
         DeformationPotential(Minimum ekp hkp)
      )
   )
}
```

The surface name specifies the surface or interface that causes the mobility degradation, for example, the silicon–oxide interface in a MOS transistor. The surface must be defined in the `Math` section of the command file. For more detailed explanations of the high-k mobility degradation models, see Chapter 5 on page 23.

Path D: FinFET Simulations – Use Path C

The same `Physics` section as in Path C can be used. As a starting point for calibration, the same parameter file `CMOS.par` can be used as well. However, because the interface quality of the fin sidewalls can be very different from the interface quality of a planar transistor, parameter adjustments are often necessary.

In general, it is observed that the FinFET electron inversion mobility is higher at the (110) sidewalls than in planar (110) transistors [1].

Table 3 shows the current approach for modeling planar and nonplanar FinFET devices regarding orientation-related parameters.

Table 3 Modeling planar and nonplanar FinFET devices

Device	Number of conducting planes	Conducting plane orientation	Channel orientation	Parameter set
Planar MOS	1	(100)	<100>	`CMOS.par`
Planar MOS	1	(110)	<100>	`CMOS.par`
Planar MOS	1	(110)	<110>	`CMOS.par`
FinFET	3	(100)	<100>	`CMOS.par`
FinFET	3	(100) (110)	<110> <110>	`CMOS.par` (but for electrons use (100) parameters for (110) as well)

Path E: Thin-Layer MOS Simulations – Inclusion of Thin-Film Effects

The `Enormal` command in the `Mobility` section of Path C must be replaced with `ThinLayer`. All other options and statements remain the same.

Path F: GaN HEMT Simulations

For numeric reasons, the well-known extended Canali model is used to simulate high-field effects. The use of the transferred electron model requires more evaluation and testing.

It is known that the surface roughness at interfaces to the GaN channel influences the channel mobility. However, because of missing model parameters and the need for further investigation of the mobility in the 2D electron gas, the model is not included here. Typically, it is advisable to use the density gradient model for quantum correction. For numeric reasons, this model is not included here.

The values for the trap concentration and the energy level are typical for nitride-passivated GaN HEMTs. However, the actual values used depend on the device and can be different from the values presented here.

In the example command file section below, the parameter file `WBG.par`, which contains the material parameters for several wide-bandgap materials, is loaded. The same parameters are also available in the parameter files `GaN.par`, `AlGaN.par`, and `AlN.par`.

```
Files {
   Parameters="$STROOT/tcad/$STRELEASE/lib/sdevice/MaterialDB/WBG.par"
   ...
}

Physics {
   Mobility (
      DopingDependence(Arora)
      HighFieldSaturation
   )
   EffectiveIntrinsicDensity(noBandGapNarrowing)
   Piezoelectric_Polarization(strain)
   Recombination(SRH Radiative)
   Fermi
   Thermodynamic
   Thermionic
   eBarrierTunneling "STUN"
   eBarrierTunneling "DTUN"
}

Physics (MaterialInterface="AlGaN/Nitride") {
   Traps(Donor Level Conc=1E13 EnergyMid=0.4 FromMidBandGap)
            # The value for the trap concentration is a calibration parameter.
   Piezoelectric_Polarization(strain activation=0)
}
```

Path G: SiC Diode Simulations

```
Files {
   Parameters="$STROOT/tcad/$STRELEASE/lib/sdevice/MaterialDB/WBG.par"
   ...
}

Physics {
   Mobility (
      DopingDependence(Arora)
      HighFieldSaturation
      IncompleteIonization
   )
   EffectiveIntrinsicDensity(oldSlotboom noFermi)
   IncompleteIonization
   Recombination(SRH(DopingDep TempDep Tunneling) Band2Band Avalanche)
   Fermi
   Thermodynamic
   AnalyticTEP
   Traps (
      Donor Level EnergyMid=1.0 FromConductionband Conc=1e14
      eXSection=1.0e-12 hXSection=1.0e-12 PooleFrenkel TrapVolume=1.0e-9
      HuangRhys=0.1 PhononEnergy=0.05 eBarrierTunneling (Twoband)
   )
}

Physics (Electrode="top") {
   Schottky BarrierLowering
   Recombination(eBarrierTunneling(Twoband Transmission)
}
```

Depending on how the mobility model has been calibrated, that is, if the total chemical concentration or the active concentration has been used, the `IncompleteIonization` statement can be added to the `Mobility` section.

The command file section is not designed and tested for breakdown simulation.

The values for the trap concentration, the energy levels, and other parameters in the trap command are typical. However, the actual values depend on the device and can be different from the values presented here.

The use of the `NoFermi` statement depends on the extraction of the bandgap narrowing model parameters. `NoFermi` is applied if you use parameters for bandgap narrowing that have been extracted assuming Fermi statistics.

An alternative option that is physically more suited – the `JainRoulston` model – can be used for bandgap narrowing. This option requires further testing and evaluation.

References

[1] C. D. Young *et al*., "(110) and (100) Sidewall-oriented FinFETs: A performance and reliability investigation," *Solid-State Electronics*, vol. 78, pp. 2–10, December 2012.

CHAPTER 4 Guide for Calibration of Device Simulations

This chapter provides an introduction to device calibration.

The basic calibration methodology used to improve the accuracy of the simulation of CMOS devices is explained here.

Calibration Methodology

This section introduces basis aspects of the CMOS calibration methodology.

Calibration of Planar CMOS Devices with Silicon Channel

Figure 1 shows a general flow of the calibration methodology used for CMOS devices. The different measurements and layout configurations allow you to separate device simulation model parameters. However, in many cases, iterations are necessary. In the next sections, this calibration methodology is explained in detail. For that, it is assumed that all process calibration issues are solved beforehand and the doping profile is correct.

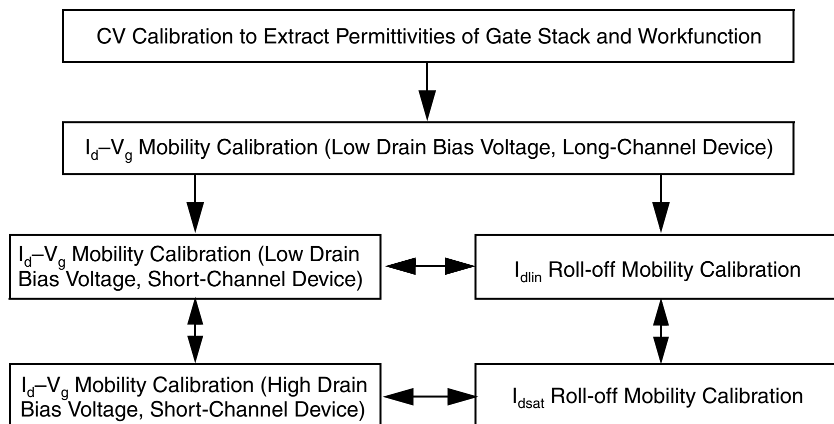

Figure 1 Calibration methodology

CV Calibration

CV calibration is the first step in the device calibration hierarchy. CV calibration is strongly connected to the doping profile and to process simulation or calibration. Because it is assumed that the doping profile is correct, the bottom of the C–V curve (region A in Figure 2) fits the experiment already. CV calibration is performed on large-area MOS transistors or MOS capacitor test structures. Table 4 lists the main steps and the extracted parameters of a CV calibration.

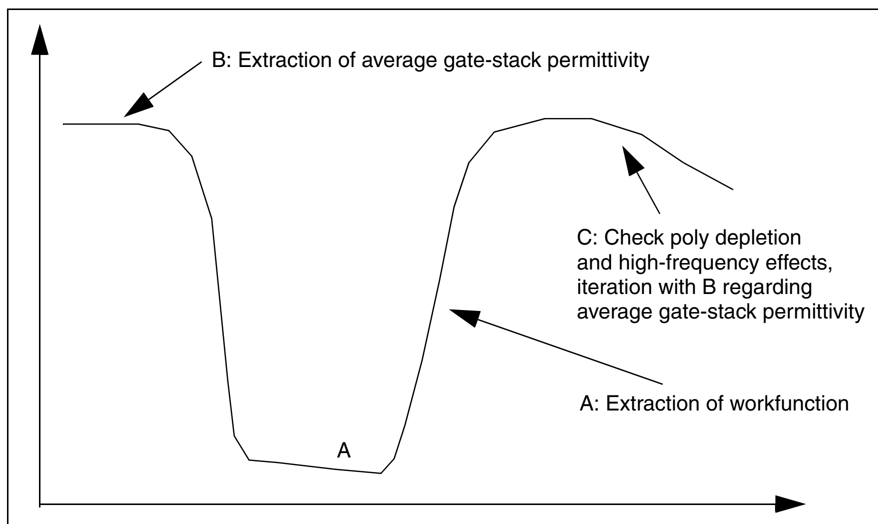

Figure 2 CV calibration methodology

Table 4 Main steps of CV calibration

Step	Target	Parameter to extract	Validity range of parameter	Comments
A	Region of weak or moderate inversion	Workfunction	Metal gate workfunction: NMOS (4.0–4.5 eV) PMOS (4.6–5.0 eV) Polygate barrier: –0.2 V – 0.2 V	Workfunction or barrier voltages extracted from CV and used for long-channel I–V simulation can require corrections, particularly in cases where special CV test structures are used.
B	Accumulation part of CV	Average permittivity of gate isolation	Permittivity of high-k material: 14–25 Permittivity of interfacial oxide: 3.9–6	In the case of high-k gate stacks with several material layers, first the permittivity of the interfacial oxide layer is adjusted. Then, the permittivity of the high-k material is calibrated.
C	Inversion part of CV	Poly doping in case of polygate	Depends on process conditions	

Long-Channel Id–Vg Calibration

The calibration of long-channel devices is necessary to extract low-field mobility parameters. Typically, I_d–V_g characteristics of devices with a gate length greater than 500 nm, at low drain bias voltage smaller than 100 mV, are used for this. The parameters of the mobility model are extracted in different voltage regions using an iterative process (see Figure 3, Figure 4, and Table 5 on page 18).

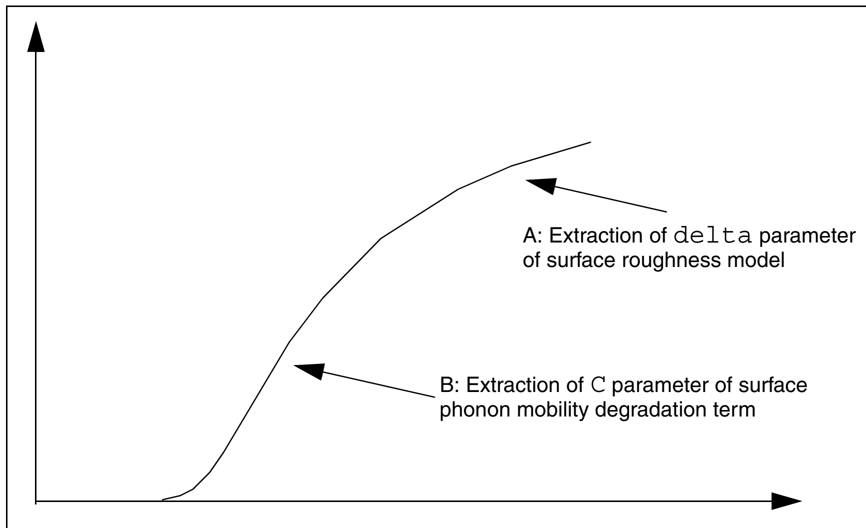

Figure 3 Long-channel I_d–V_g calibration methodology (linear scale)

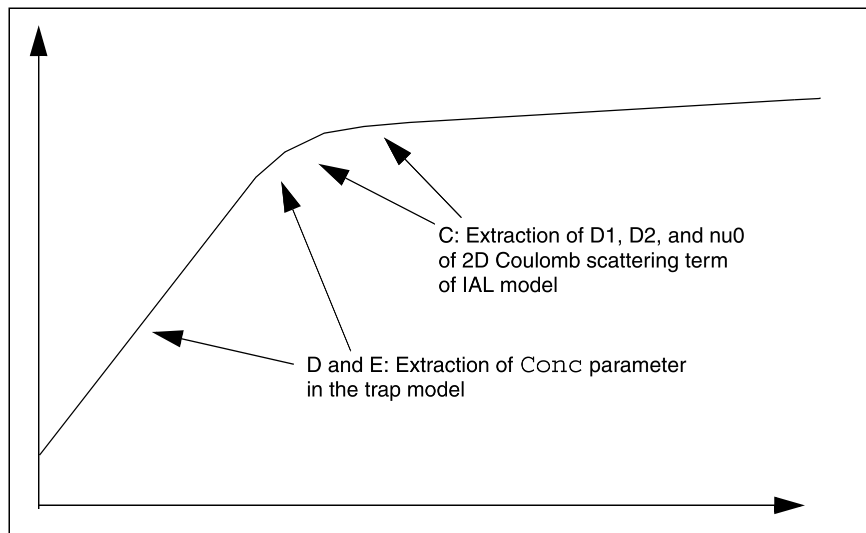

Figure 4 Long-channel I_d–V_g calibration methodology (logarithmic scale)

Table 5 Main steps of long-channel I_d–V_g calibration

Step	Target	Parameter to extract	Validity range of parameter	Comments
A	Threshold voltage	Workfunction	Depends on gate material	Typically, metal gate workfunctions of 4.1 eV for NMOS and 4.9 eV for PMOS are taken. Take initial value from CV calibration. Note there can be an influence of remote Coulomb scattering (RCS) or 2D impurity Coulomb scattering on the threshold voltage, which couples workfunction and mobility extraction.
B	Strong inversion – high gate bias voltage	`Delta` parameter of surface roughness model	Depends on process conditions and other parameters – no validity range known	Surface roughness can change when changing process conditions and surface orientations. Fine-tuning is always necessary to fit I_d–V_g characteristics.
C	Linear region of I_d–V_g curve	`C` parameter of surface phonon mobility degradation term	Depends on process conditions and other parameters – no validity range known	The extraction requires mostly an iteration between B and C and, sometimes, even between B, C, and D. Interface properties and material composition at the interface can change when changing process conditions. Fine-tuning is always necessary to fit I_d–V_g characteristics.
D	Transition between logarithmic and linear slope – threshold voltage region	1. Parameters of 2D Coulomb mobility degradation term 2. Parameters of InterfaceCharge model	1. No validity range known 2. No validity range known	Calibration focuses on the Coulomb roll-off visible in the $\mu(E_{eff})$ curve, but it also can be done to the bending of the I_d–V_g curve between subthreshold and linear region. These mobility degradation terms also affect the threshold voltage and the DIBL of the device.
E	Subthreshold region	Parameters of InterfaceCharge model	No validity range known	Calibration focuses on the Coulomb roll-off visible in the $\mu(E_{eff})$ curve, but it also can be done to the subthreshold region. This mobility degradation term also affects the threshold voltage and the drain-induced barrier lowering (DIBL) of the device.

Table 5 Main steps of long-channel I_d–V_g calibration

Step	Target	Parameter to extract	Validity range of parameter	Comments
F	Leakage current region	Band-to-band tunneling model and Shockley–Read–Hall (SRH) recombination generation model	No validity range	Calibration depends on the physical mechanism ('electrostatic' punch-through, band-to-band tunneling, SRH contributions).

Short-Channel Id–Vg Calibration at Low Drain Bias

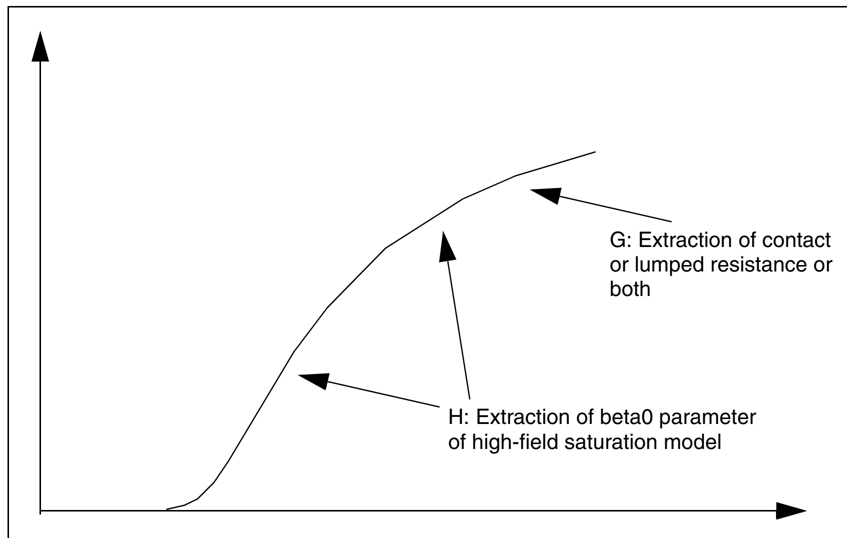

Figure 5 Short-channel I_d–V_g calibration methodology (linear scale, low drain bias voltage)

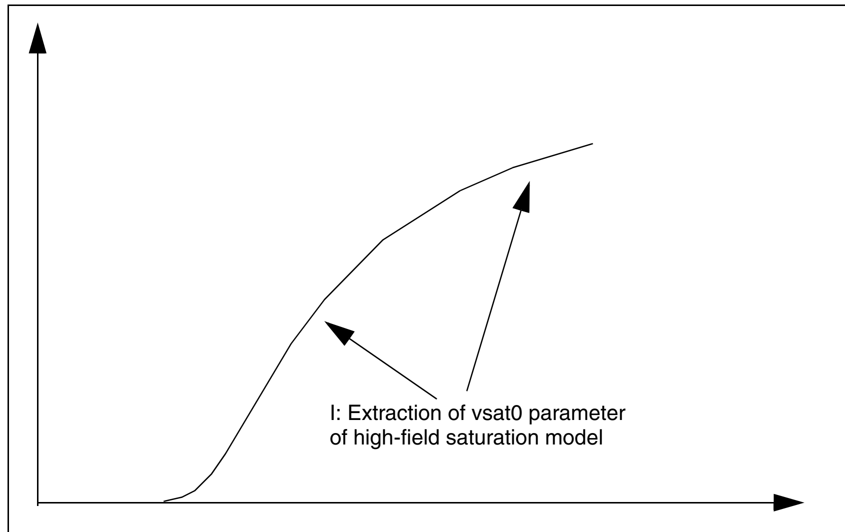

Figure 6 Short-channel I_d–V_g calibration methodology (linear scale, high drain bias voltage)

Table 6 Short-channel I_d–V_g calibration for low drain bias voltage

Step	Target	Parameter to extract	Validity range of parameter	Comments
G	Strong inversion – high gate bias voltage	External lumped resistance, contact resistance, source/drain – extension resistance	No validity range	Iteration with H.
H	Moderate inversion – g_m region	Check influence of resistances and adjust `beta0` parameter	No validity range	Iteration with I and G.

It is not possible to perform a physically sound calibration of the current response at high-driving fields (saturation current in MOSFETs controlled by the saturation velocity) and low-driving fields (linear regime of a MOSFET), at the same time, when having strong built-in fields (fields that are present without having any currents, for example, at the p-n junction) and ballistic effects. This is connected with the overestimated current response close to equilibrium [1] and the known velocity overshoot effects.

There are some workarounds such as introducing gate length–dependent low-field mobility, performing a different saturation velocity calibration for different drain bias voltages, or

calibrating `vsat0` and `beta0` at the same time, and accepting strong changes of the default values. These approaches can help to achieve a certain accuracy but do not solve the problem.

One hypothesis links the current overestimation close to equilibrium with the validity of the Einstein relation when leaving the equilibrium at strong built-in fields. An implementation in Sentaurus Device that allows you to break the Einstein relation has been used to support this hypothesis. However, strong numeric problems and a lack of physical understanding do not allow this implementation to be defined as a standard approach. More numeric and physical investigations are needed.

Short-Channel Id–Vg Calibration at High Drain Bias

In this step, saturation velocity is extracted.

Table 7 Short-channel I_d–V_g calibration for high drain bias

Step	**Target**	**Parameter to extract**	**Validity range of parameter**	**Comments**
I	Whole I_d–V_g curve and I_{dsat}	Adjust `vsat0`	For silicon: < 3e7 cm/s	Iteration with `beta0` extraction (H) may be necessary.

The extraction of `vsat0` from I_{dsat} roll-off data or I_d–V_g curves at large drain bias voltage, using experiments or Monte Carlo (MC) simulation, is mostly straightforward. However, the calibration of both I_{dsat} and I_{dlin} at the same time using `vsat0` and source/drain resistance only, without worsening the shape of the I–V curves, is difficult. Including `beta0` in this calibration can help to circumvent these problems. The parameter `beta0` influences especially the range of moderate fields, but it does not act in complete saturation where `vsat0` determines the strongly saturated region. Therefore, you can try to adjust I_{dsat} mainly with `vsat0` and I_{dlin} mainly with `beta0`. Iteration between both parameters is mostly necessary.

The following examples (see Table 8 and Table 9 on page 22) show the adjustment of `vsat0` to match the MC-simulated I_{dsat} roll-off curve for a PFinFET device for channel germanium mole fractions of 0% and 35%. I_{dsat} can be matched perfectly to MC simulation by adjusting `vsat0`, where 35% Ge requires a higher `vsat0` value than for the pure silicon channel. Despite the lower physical velocity saturation and the lower low-field mobility because of alloy scattering, ballistic transport seems to increase with the mole fraction, resulting finally in a higher I_{dsat} value.

It is obvious I_{dlin} is much too high for the short-channel devices where I_{dsat} matches well the MC simulation result. Optimizing `vsat0` and `beta0` together could result in a better fit for both I_{dlin} and I_{dsat}.

Table 8 Calibration of I_{dsat} (vsat0 = 1.1e07 cm/s, default: 8.4e06 cm/s) for <110> silicon channel PFinFET

Gate length [nm]	I_{dsat} MC [μA/μm]	I_{dsat}	I_{dlin} MC [μA/μm]	I_{dlin}
15	454	450	126	183
60	164	179	58	74
100	119	128	40	49

Table 9 Calibration of I_{dsat} (vsat0 = 1.7e07 cm/s, default: 7.5e06 cm/s) for <110> channel 35% SiGe PFinFET

Gate length [nm]	I_{dsat} MC [μA/μm]	I_{dsat}	I_{dlin} MC [μA/μm]	I_{dlin}
15	396	424	100	143
60	117	131	44	50
100	80	86	30	31

References

[1] A. T. Pham, C. Jungemann, and B. Meinerzhagen, "Modeling and validation of piezoresistive coefficients in Si hole inversion layers," *Solid-State Electronics*, vol. 53, no. 12, pp. 1325–1333, 2009.

CHAPTER 5 Review of Models

This chapter provides a review of selected models of Sentaurus Device.

Overview of Models

Given the large number of different models developed and implemented in Sentaurus Device for the simulation of device characteristics, it is often difficult to quickly design appropriate command files for device simulation. Therefore, this chapter presents a review of selected models, and the models are evaluated with respect to their capabilities in simulating certain device aspects.

In the quantum drift-diffusion (QDD) approximation, charge carrier transport is determined by the electron and hole mobilities. Version H-2013.03 of Advanced Calibration Device focuses on low-field mobility and high-field mobility, with and without mechanical stress, for planar and nonplanar silicon and SiGe FETs. A discussion of models and parameters for GaN and SiC devices is presented as well.

CMOS Devices

Unstrained Band Structure and Electrostatics

In Sentaurus Device, the bulk band structure is defined by the band gap, the electron affinity, the bandgap narrowing, and the density-of-states (DOS). The temperature dependency of these quantities and the doping dependency of the bandgap narrowing are represented by empirical functions. The parameters of these functions are in the Advanced Calibration Device parameter files.

Strained Band Structure and Electrostatics

The band structure changes with the mechanical stress in the device. The dependency of the conduction and valence bands and, therefore, of the band gap and electron affinity, on the mechanical stress or strain is described by the deformation potential model where the band structure information comes from $k \cdot p$ calculation. The stress dependency of the DOS can be

extracted from $k \cdot p$ calculation as well. The parameters for these models are in the Advanced Calibration Device parameter files.

Unstrained Low-Field Mobility

In the limit of low-driving fields, the mobility is degraded by several mechanisms. Typically, MISFET simulation takes into account mobility degradation by ionized dopants, surface roughness, surface phonon, and bulk phonon scattering. For high-k gate stacks, additional remote scattering mechanisms such as remote Coulomb scattering (RCS), remote phonon scattering (RPS), and remote dipole scattering (RDS) must be considered. A crucial point is the transition between bulk mobility and inversion or accumulation layer mobility. Because of the transition from 3D to 2D charge carrier gas, the scattering behavior of electrons and holes changes and screening becomes different. Furthermore, the mobility model must include the dependency on the channel material, which means for example on the germanium mole fraction, and on the channel and surface or interface orientations. For thin silicon films in the range of a few nanometers, additional contributions come into effect that cause a dependency of the mobility on the film thickness.

In summary, a drift-diffusion or QDD low-field mobility model for the simulation of SiON/SiO_2 or high-k gate stack FETs without mechanical stress should have the following features:

- Mobility degradation by ionized impurities – impurity Coulomb scattering (ICS)
- Mobility degradation by the roughness of the surface or interface – surface roughness scattering (SRS)
- Mobility degradation by interaction with bulk phonons – bulk phonon scattering (BPS)
- Mobility degradation by interaction with surface phonons – surface phonon scattering (SPS)
- Mobility degradation by charges in the gate isolator (high-k gate stack) (RCS)
- Mobility degradation by different permittivity in the gate isolator (high-k gate stack) (RPS)
- Mobility degradation by dipole configurations in the gate isolator (high-k gate stack) (RDS)
- Mole fraction dependency of the low-field mobility model parameters
- Transition between bulk scattering and scattering in 2D charge carrier gas for ICS
- Parameters for different channel and surface or interface orientations (channel: <100> and <110>; surface: (100) and (110))
- Mobility degradation for very thin silicon films
- Including influence of quantization on mobility in thin films

Eq. 1 gives the corresponding formulation of the low-field mobility model using Mathiessen's rule:

$$\frac{1}{\mu} = \frac{1}{f_t \cdot \mu_{ICS3D} + (1 - f_t) \cdot \mu_{ICS2D}} + \frac{1}{\mu_{BPS}} + \frac{f_{tf}(\mu_{SPS})}{\mu_{SPS}} + \frac{1}{\mu_{SRS}} + \frac{1}{\mu_{RCS}} + \frac{1}{\mu_{RPS}} + \frac{1}{\mu_{RDS}} + \frac{1}{\mu_{TF}} \quad (1)$$

where f_t is the transition function between Coulomb scattering in 3D and 2D charge carrier gas; it is defined in the *Sentaurus Device User Guide*. f_{tf} is the quantization function describing the influence of the film thickness on the phonon scattering; it can be derived from the *Sentaurus Device User Guide*.

Sentaurus Device offers low-field mobility degradation models for MISFET simulation:

- Bulk phonon-limited mobility model (BPS):

  ```
  Physics { ConstantMobility }
  ```

- Mobility degradation by ionized impurities (in some cases, it contains, in the low-doping limit, the bulk phonon-limited mobility) (ICS):

  - Masetti model: Provides mole fraction–dependent model parameters:

    ```
    Physics { Mobility ( DopingDependence (Masetti) ) }
    ```

  - Arora model: Provides mole fraction–dependent model parameters:

    ```
    Physics { Mobility ( DopingDependence (Arora) ) }
    ```

  - Philips unified mobility model (`PhuMob`): Includes screening and carrier–carrier scattering, and provides mole fraction–dependent model parameters:

    ```
    Physics { Mobility (PhuMob) }
    ```

  - University of Bologna bulk mobility model: Specially calibrated for an extended temperature range and provides mole fraction–dependent model parameters:

    ```
    Physics { Mobility ( DopingDependence (UniBo2) ) }
    ```

  - Carrier–carrier scattering models (Conwell–Weisskopf and Brooks–Herring):

    ```
    Physics { Mobility (CarrierCarrierScattering) }
    ```

- Mobility degradation at interfaces:

  - Enhanced Lombardi model: Includes automatic detection of surface orientation and provides mole fraction–dependent model parameters:

    ```
    Physics { Mobility ( Enormal (Lombardi) ) }
    ```

  - Enhanced Lombardi model with high-k degradation (`Lombardi_highk`) including RCS and RPS:

    ```
    Physics { Mobility ( Enormal (Lombardi_highk) ) }
    ```

- Inversion and accumulation layer mobility model (`IALMob`): Includes automatic detection of surface orientation, provides mole fraction–dependent model parameters, and contains Philips unified mobility model, enhanced Lombardi model, and additional terms for Coulomb scattering in 2D electron gas:

```
Physics { Mobility ( -ConstantMobility Enormal (IALMob) ) }
```

- University of Bologna surface mobility model: Specially calibrated for an extended temperature range, includes screening of bulk ICS, no special model for ICS in 2D charge carrier gas, simplified Lombardi-style model for acoustic phonon and surface roughness scattering:

```
Physics { Mobility ( Enormal (UniBo) ) }
```

- 2D Coulomb scattering model for ionized impurities: Must not be used together with `PhuMob` or any other `DopingDependence` model because mobility degradation is double counted; designed for Coulomb scattering (ICS) in 2D charge carrier gas:

```
Physics { Mobility ( Enormal (Lombardi Coulomb2D) ) }
```

- 2D Coulomb scattering models for positive and negative charges at remote interfaces: Is used to replace the `Lombardi_highk` RCS terms, has better numerical behavior and gives the possibility to distinguish between RCS and RDS:

```
Physics { Mobility ( Enormal (Lombardi NegInterfaceCharge
   PosInterfaceCharge) ) }
```

- Thin-layer mobility model (`ThinLayer`): Describes mobility degradation due to finite silicon film thickness, includes dependency of phonon scattering on quantization but also additional empirical mobility degradation terms, and includes automatic detection of surface orientation:

```
Physics { Mobility (ThinLayer) }
```

Because of the use of Mathiessen's rule, several combinations of the above mobility models are possible. For MISFETs, you usually need to combine bulk phonon and Coulomb scattering with scattering at interfaces and surfaces. Historically, the following combinations have been used:

1. `DopingDependence(Masetti)` + `Lombardi`
2. `PhuMob` + `Lombardi_highk` or `Lombardi`
3. `IALMob`
4. `IALMob` + `Lombardi_highk`
5. `IALMob` + `Lombardi_highk` + `NegInterfaceCharge` + `PosInterfaceCharge`
6. `IALMob` + `Lombardi_highk` + `NegInterfaceCharge` + `PosInterfaceCharge` + `ThinLayer`

Model combination 2 has been used for a long time as the standard model. However, several problems call for a change to another low-field mobility model. First, the transition between 3D bulk Coulomb scattering and Coulomb scattering in the inversion layer is not correctly described because the `PhuMob` model, which is a bulk model, is used for the mobility degradation by scattering at ionized impurities from accumulation to strong inversion. This causes problems in describing the onset of the moderate or strong inversion around the threshold voltage in the I_d–V_g curve. Second, the dependency on the amount of remote interface charge and the distance between the remote charge and the charge carrier are not treated well in the `Lombardi_highk` model. Third, in thin silicon layers, it is mandatory to include the dependency on the film thickness.

NOTE For these reasons, it is necessary to change the low-field mobility framework and to switch to model combination 3, 5, or 6. The recommended models for MISFET simulation are model 3 (devices without high-k gate stacks), model 5 (devices with high-k gate stacks), and model 6 (thin films).

Strained Low-Field Mobility

Influence of Mechanical Stress

The modeling of the stress influence on the channel mobility must deal with several typical configurations. These configurations must be simulated accurately with the goal to minimize additional device calibration. The typical cases are:

- Planar PMOS with compressive stress between 0.5 GPa and 2 GPa in the channel direction and up to 2 GPa tensile stress normal to the silicon surface (gate-first with SiGe pockets and dual stress liner (DSL)).
- Planar PMOS with compressive stress between 1 GPa and 3 GPa in the channel direction and less than 500 MPa normal to the silicon surface (gate-last with SiGe pockets).
- Planar NMOS with tensile stress between 1 GPa and 2 GPa in the channel direction and less than 500 MPa normal to the silicon surface (gate-last with SiC pockets).
- Planar NMOS with tensile stress between 300 MPa and 1.5 GPa in the channel direction and up to 2 GPa compressive stress in the normal direction (gate-first with DSL and stress memorization technique).
- Planar PMOS with biaxial strained SiGe channel and stress between 1 MPa and 4 GPa in the channel direction and up to 2 GPa tensile stress in the normal direction (gate-first with DSL and SiGe pockets).
- Nonplanar NMOS (FinFET) with mixed compressive or tensile stress components of up to 2 GPa depending on the configuration (for example, with SiC pockets wrapped around the fin and metal gate as a liner replacement).

- Nonplanar PMOS (FinFET) with mixed compressive or tensile stress components of up to 2 GPa depending on the configuration (for example, with SiGe pockets wrapped around the fin and metal gate as a liner replacement).

The stress configurations must be simulated for several wafer orientations (for example, (001) and $(1\underline{1}0)$), channel directions (for example, <100> and <110>), and channel materials (for example, silicon and SiGe). Typically, all three stress components S_{xx}, S_{yy}, and S_{zz} are important. A model validity check, which is limited to uniaxial or biaxial stress configurations, is not sufficient. In addition, the response of the mobility degradation components (such as phonon scattering, Coulomb scattering, and remote scattering) to mechanical stress is different and requires the separate treatment of each component. This approach results in the following equation:

$$
\begin{aligned}
\frac{1}{\mu} = {} & \frac{1}{f_t \cdot (1 + p_{0,\,\mathrm{ICS3D}}) \cdot \mu_{0,\,\mathrm{ICS3D}} + (1 - f_t) \cdot (1 + p_{0,\,\mathrm{ICS2D}}) \cdot \mu_{0,\,\mathrm{ICS2D}}} + \frac{1}{(1 + p_{0,\,\mathrm{BPS}}) \cdot \mu_{0,\,\mathrm{BPS}}} \\
& + \frac{1}{(1 + p_{0,\,\mathrm{SPS}}) \cdot \mu_{0,\,\mathrm{SPS}}} + \frac{1}{(1 + p_{0,\,\mathrm{SRS}}) \cdot \mu_{0,\,\mathrm{SRS}}} + \frac{1}{(1 + p_{0,\,\mathrm{RCS}}) \cdot \mu_{0,\,\mathrm{RCS}}} \\
& + \frac{1}{(1 + p_{0,\,\mathrm{RPS}}) \cdot \mu_{0,\,\mathrm{RPS}}} + \frac{1}{(1 + p_{0,\,\mathrm{RDS}}) \cdot \mu_{0,\,\mathrm{RDS}}}
\end{aligned}
\qquad (2)
$$

with $p_{0,\,\mathrm{ICS3D}}$ as the mobility enhancement factor for the mobility limited by scattering at ionized impurities in a 3D bulk situation and for the other p_0 terms similarly. Currently, this treatment of the scattering terms is not possible in Sentaurus Device; instead, the total mobility is scaled with a stress enhancement factor calculated with the models discussed below. The models describing the influence of stress on the mobility available in Sentaurus Device are:

- First-order (linear) piezoresistance mobility model
- Second-order piezoresistance mobility model
- Nonlinear piezoresistance model for electrons and holes (`MCmob`)
- Intel stress-induced hole mobility model (`hSixBand`)
- `eSubband` model for electrons
- `hSubband` model for holes

Several additional options can be chosen. For the piezoresistance models, the `Kanda` option includes the dependency of the stress-induced mobility change on the doping concentration. Differences in the influence of mechanical stress on minority and majority carriers can be considered by an additional fitting parameter. In addition, you can calibrate the influence of the normal electric field in a MIS structure and of the germanium mole fraction on the first-order piezo coefficients. Because the linear piezoresistance model is a bulk model, the default piezoresistance coefficients are not accurate for inversion layers and must be adjusted. The piezoresistance model can be used as a factor model or a tensor model, in this way, introducing anisotropic properties.

The influence of the saturation velocity on the stress-dependent mobility can be fine-tuned by a parameter that controls how strongly the saturation velocity depends on the stress. Setting this parameter to zero means the mobility change is applied to the low-field mobility only. Setting the parameter to 1, which is the default in Sentaurus Device, means the mobility change is applied to the total mobility. Because it is known from MC simulation and from experiments that short-channel transistors show a much lower mobility enhancement due to mechanical stress, it is better to apply the mobility change to the low-field mobility only. Further adjustment of this parameter should be performed with good references only.

The occupation-based and band structure–based models (`eSubband` and `hSubband` models, and Intel model) have their own dependency on the doping concentration, and a `Kanda`-like option is not necessary. In addition, the electric field dependency should be a result of the model itself.

The following sections describe the models and options, and give some information about problems and advantages.

Piezoresistance Mobility Models

First-Order (Linear) Piezoresistance Mobility Model

This model uses the piezoresistance tensor with constant coefficients to calculate the stress-induced mobility change.

Options:

It can be used as a factor (isotropic) model or a tensor (anisotropic) model. The piezoresistance coefficients can depend on the normal electric field in an inversion layer. Minority and majority charge carrier transport can be distinguished. Dependency on the doping concentration can be included. Calibration of dependency of the influence of mechanical stress on the velocity saturation is possible.

Advantages:

The model is well adjusted to measurements for the bulk case. It is fully transformable, making it possible to consider all stress configurations and current directions in a bulk situation. It is easy to use and to calibrate.

Problems:

Accurate for low stress only (< 200 MPa). Tensor symmetry is broken for nonbulk conditions as in an inversion layer, which is not reflected by the model. Default piezoresistance coefficients are not accurate for inversion layers.

Second-Order Piezoresistance Mobility Model

This model uses the 6th-grade piezoresistance tensor with constant coefficients to calculate the stress-induced mobility change.

Options:

The model can be used as a factor (isotropic) model or a tensor (anisotropic) model. Minority and majority charge carrier transport can be distinguished. Dependency on the doping concentration can be included. Calibration of dependency of the influence of mechanical stress on the velocity saturation is possible.

Advantages:

Parameters are available for the bulk case. The model is fully transformable, making it possible to consider all stress configurations and current directions in a bulk situation.

Problems:

Accurate for low and moderate stress values only (< 500 MPa). Tensor symmetry is broken for nonbulk conditions as in an inversion layer, which is not reflected by the model. Default piezoresistance coefficients are not accurate for inversion layers.

Nonlinear Piezoresistance Model for Electrons and Holes (MCmob)

This model can use nonlinear piezoresistance coefficients and higher-order cross-term corrections that are extracted from MC simulation, Sentaurus Band Structure simulation, or other sources (experiments and simulations available from the literature).

Options:

Minority and majority charge carrier transport can be distinguished. Dependency on the doping concentration can be included. Calibration of dependency of the influence of mechanical stress on the velocity saturation is possible. Germanium mole fraction dependency of the model coefficients can be switched on. Parameters for different orientations can be used and an auto-orientation option is available. Complete parameter sets can be loaded using the Sentaurus Device parameter file.

Advantages:

Parameters are available for strong inversion and for different channel materials (silicon and SiGe). The model can be extended to other conditions when there are reference tools such as MC simulations or experiments. Available for different channel and wafer orientations. The model is fast and can be calibrated easily.

Problems:

Interpolation especially for untypical stress conditions must always be validated. The physics is in the reference tool, for example, the MC simulator. Improvement of the model without improving the reference tool or without obtaining better experiments is, except with respect to the interpolation, not possible. The settings for the local coordinate system must be specified in the Sentaurus Device parameter file.

Occupation-based and Band Structure-based Models

The models in this section characterize the dependency of occupation and band structure on mechanical stress for the calculation of the mobility.

Intel Stress-induced Hole Mobility Model (hSixBand)

This model uses the change of band structure and occupation to calculate stress-dependent mobility.

Options:

Dependency on the doping or carrier concentration can be switched on.

Advantages:

The model is derived from physical assumptions.

Problems:

Calibration is not straightforward. Only silicon as a channel material is available. The influence of surface orientation cannot be described. The model has been developed and calibrated for uniaxial stress in the <110> direction. The combination of the component normal to the MIS plane with the in-plane stress components is not validated.

eSubband Model for Electrons

This model uses a change of band structure and occupation to calculate the mobility change.

Options:

Dependency on the doping or carrier concentration can be switched on. Stress-related change in the scattering can be included. Change of effective mass with stress can be added to the model. For the inversion layer, the `MLDA` option can be used.

Advantages:

The modified local-density approximation (MLDA) allows you to move from bulk to inversion layer conditions, and to take surface or channel orientation dependency into account. The model is derived from physical assumptions. The model is validated and calibrated for silicon for different channel and surface orientations.

Problems:

Calibration is not straightforward. Only silicon as a channel material is available.

hSubband Model for Holes

This model uses a change of band structure and occupation to calculate stress-dependent mobility.

Options:

Dependency on the doping or carrier concentration can be switched on. Stress-related change in the scattering can be included. Change of effective mass with stress can be added to the model. For the inversion layer, the `MLDA` option can be used.

Advantages:

MLDA allows you to move from bulk to inversion layer conditions, and to take surface or channel orientation dependency into account. The model is derived from physical assumptions. The model is validated and calibrated for silicon for different channel and surface orientations.

Problems:

Calibration is not straightforward. Only silicon as a channel material is available.

Unstrained High-Field Mobility

The low-field mobility models are valid for small driving forces only. To take into account high-field effects, an additional model – the high-field saturation model – is introduced in the drift-diffusion model framework. The high-field saturation model should limit the velocity-field relation to the saturation velocity of the material when having sufficient scattering, and it must provide a way to calibrate the influence of quasiballistic and ballistic transport on the charge carrier transport. In addition, it should give the possibility to calibrate the germanium mole fraction dependency of the model parameters. Furthermore, because of deficiencies in the drift-diffusion model to describe the current response close to equilibrium, a model is needed that gives the possibility to compensate or, at least, to calibrate for this deficiency.

In summary, a drift-diffusion or QDD high-field mobility model for the simulation of SiON/ SiO_2 or high-k gate stack FETs without mechanical stress should have the following features:

- For unstrained cases with sufficient scattering limitation of the drift velocity to the saturation velocity for high fields.
- Possibility to calibrate the model with respect to ballistic and quasiballistic transport.
- Germanium mole fraction–dependent model parameters.
- Possibility to calibrate the model with respect to current response close to equilibrium.
- Orientation-dependent model parameters.

Sentaurus Device offers high-field mobility models for MISFET simulation:

- Extended Canali model: It is the mainstream model for drift-diffusion simulation, and it can be used with the hydrodynamic model as well. It has calibrated parameters for silicon and SiGe for situations where ballistic or quasiballistic transport is not present. Calibration to short-channel devices where quasiballistic transport occurs can be done using model parameters:

```
Physics { Mobility (HighfieldSaturation) }
```

- Transferred electron model: Specially designed for GaAs and materials with similar band structure:

```
Physics { Mobility ( HighfieldSaturation (TransferredElectronEffect) ) }
```

- Basic model: Simple model with carrier temperature as the driving force and requires the hydrodynamic model:

```
Physics { Mobility ( HighfieldSaturation (CarrierTempDriveBasic) ) }
```

- Meinerzhagen–Engl model: Canali-like high-field saturation model with carrier temperature as the variable and requires the hydrodynamic model:

```
Physics { Mobility ( HighfieldSaturation (CarrierTempDriveME) ) }
```

The common model for drift-diffusion or QDD simulations is the extended Canali model.

NOTE Calibrated mole fraction–dependent parameters are available and extensive experience exists. Numeric problems are known or are already solved.

Strained High-Field Mobility

The dependency of the high-field mobility on mechanical stress is determined, in the QDD model, by the strain dependency of the saturation velocity. The saturation velocity covers in this model both the strain dependency of the physical saturation velocity and the strain

dependency of the quasiballistic transport. The model is again the Canali model where the parameter `saturationfactor` controls the stress dependency.

Gallium Nitride HEMTs

GaN HEMTs have unique qualities that require special attention. First, there is the large band gap that results in very low charge-carrier densities as well as numeric problems. Second, in the on-state, the current conduction is performed using a 2D electron gas channel in the GaN layer. This has implications for the modeling of the mobility. Third, most of these structures use material combinations in addition to pure GaN and AlN such as AlGaN. The mole fraction of these alloys determines the thermal conductivity, mobility, and band gap. For that, mole fraction–dependent parameters that make the transition from GaN to AlN are necessary. Mostly, linear or parabolic interpolation between GaN and AlN is not sufficient because of the alloy influence. Furthermore, there is the influence of the strain causing polarization in the device. In addition, traps heavily influence the device operation, and the velocity saturation behavior is different to silicon.

Silicon Carbide Devices

As another wide bandgap material, SiC shows some differences to silicon as well. There are again numeric problems connected with the small densities caused by the large band gap. The anisotropy of the mobility and of the avalanche coefficients is difficult to handle numerically. Traps, contact behavior, incomplete ionization, and tunneling play more critical roles than in silicon devices.

Because of the wide band gap, the incomplete ionization model (`IncompleteIonization`) must be included in the simulation. Anisotropic behavior can be considered for thermal conductivity, mobility, and impact ionization.

Silicon Smart-Power and Power Devices

The model requirements are similar to those for silicon deep-submicron devices (see Chapter 3 on page 5) fabricated by gate-first processes, but with a greater variety of process and doping conditions as well as layout specifications. In addition, there is a need for:

- High accuracy over a wide temperature range up to very high temperatures.
- Good modeling capabilities for avalanche and breakdown.
- Good modeling capabilities for electrostatic discharge (ESD).

For avalanche, the new University of Bologna impact ionization model (`UniBo2`) is calibrated for a temperature range from 300 K to 773 K and is, therefore, best suited for ESD and high-temperature simulations. It also is recommended for room-temperature breakdown simulations.

CHAPTER 6 Parameter Files

This chapter discusses the features of the parameter files.

The information presented here relates to the models presented in Chapter 3 on page 5 and to the files AlN.par, AlGaN.par, GaN.par, 4H-SiC.par, 6H-SiC.par, CMOS.par, and WBG.par that are stored in the MaterialDB folder of Sentaurus Device.

Content of Parameter Files

The file CMOS.par must be loaded when simulating silicon or SiGe CMOS, silicon smart-power, or silicon power devices.

The files AlN.par, AlGaN.par, and GaN.par must be loaded when simulating wide-bandgap III–V nitride devices. The file 4H-SiC.par or 6H-SiC.par must be loaded when simulating SiC devices. Alternatively, the file WBG.par can be loaded when simulating wide-bandgap III–V nitride or SiC devices.

Table 10 lists the content and the features of the parameter files. The references, additional comments for the parameters, and corresponding Sentaurus Device command file sections can be found in the header of the parameter files.

Table 10 Content and features of parameter files

Parameter file	Material	Parameters for...
CMOS.par WBG.par	Oxide	• Permittivity • Thermal conductivity
CMOS.par WBG.par	Nitride	• Permittivity • Thermal conductivity
CMOS.par	InterfacialOxide	• Permittivity • Thermal conductivity
CMOS.par	HfO2	• Permittivity • Thermal conductivity

Table 10 Content and features of parameter files

Parameter file	Material	Parameters for...
WBG.par GaN.par	GaN	• Isotropic and anisotropic permittivity • Thermal conductivity • Lattice heat capacity • Band gap • Density-of-states (DOS) • Mobility with doping dependency and interface mobility degradation • Anisotropic mobility • High field dependency • SRH • Auger • Impact ionization • Quantum potential • Piezoelectric polarization • Energy relaxation time
WBG.par AlN.par	AlN	• Isotropic and anisotropic permittivity • Thermal conductivity • Lattice heat capacity • Band gap • DOS • Mobility with doping dependency • High field dependency • SRH • Auger • Impact ionization • Quantum potential • Piezoelectric polarization • Energy relaxation time
WBG.par AlGaN.par	AlGaN	• Mole fraction–dependent isotropic and anisotropic permittivity • Mole fraction–dependent thermal conductivity • Mole fraction–dependent band gap • Mole fraction–dependent mobility with doping dependency • Mole fraction–dependent high field dependency • SRH • Auger • Mole fraction–dependent impact ionization • Quantum potential • Mole fraction–dependent piezoelectric polarization • Energy relaxation time

Table 10 Content and features of parameter files

Parameter file	Material	Parameters for...
WBG.par 4H-SiC.par 6H-SiC.par	SiC	• Isotropic and anisotropic permittivity • Isotropic and anisotropic thermal conductivity • Lattice heat capacity • Band gap and bandgap narrowing • DOS • Mobility with doping dependency and interface mobility degradation • Anisotropic mobility • Isotropic and anisotropic high field dependency • SRH • Auger • Isotropic and anisotropic impact ionization • Incomplete ionization
CMOS.par	Si	• Permittivity • Thermal conductivity • Band gap and bandgap narrowing • DOS • Bulk and inversion mobility for different surface and channel orientations • High field dependency • Mechanical compliance • Deformation potential and $k \cdot p$ parameters
CMOS.par	SiGe (0–100%) can be used for Ge as well	• All models are mole fraction dependent • Permittivity • Thermal conductivity • Band gap and bandgap narrowing • DOS • Bulk and inversion mobility for different surface and channel orientations • High field dependency • Mechanical compliance • Deformation potential and $k \cdot p$ parameters (mole fraction dependency is extracted up to 50%)
CMOS.par	Ge	• Permittivity • Thermal conductivity • Band gap • DOS • Bulk mobility
CMOS.par	InGaAs	• Permittivity • Thermal conductivity
CMOS.par	GaAs	• Permittivity • Thermal conductivity
CMOS.par	InAs	• Permittivity • Thermal conductivity

CHAPTER 7 Quality of Fitting and Extraction

This chapter discusses fitting quality and extraction issues.

Low-Field Mobility of Planar CMOS Devices with Silicon Channel and Oxide–Silicon Interface

This section briefly explains how the low-field parameter sets were calibrated.

Data from Takagi *et al*. [1][2], Nakamura *et al*. [3], and Nayfeh *et al*. [4] was used for the calibration of the mobility in the transistor channel. All data is from pure polysilicon/SiO_2 gate stacks with oxide thicknesses of 25 nm for Takagi, 2 nm for Nakamura, and 5 nm for Nayfeh.

This data does not have high-k gate stacks and, therefore, allows you to extract the model parameters of surface phonon, surface roughness, and Coulomb scattering at ionized impurities. On the other hand, the process-induced variations in surface roughness and the material composition of the first atomic layers at the isolator–silicon interface can influence the mobility and result in different mobilities for different gate-formation process steps. These differences cannot be reflected by a single parameter set. Therefore, the parameter set presented here is a starting point for calibration.

Usually, the extraction of low-field mobility as a function of the effective electric field E_{eff} is performed in the following way.

First, the drain current is measured in the linear regime and, from that, the mobility is calculated for each gate voltage. At the same time, the inversion charge per area N_{inv} is calculated from C–V characteristics. Because E_{eff} is not measured, it must be calculated from N_{inv} using $E_{\mathrm{eff}} = E_{\mathrm{eff}}(N_{\mathrm{depl}}, N_{\mathrm{inv}}, \eta)$. Mostly, the depletion approximation with N_{depl} as the depletion charge is used for this, where the doping is extracted from other experiments and is assumed to be constant. The result is the dependency $\mu = \mu(E_{\mathrm{eff}})$. To obtain the universal behavior, that is, doping-independent behavior of the mobility for strong inversion, the fitting parameter η is introduced in the equation used for determining the effective field. You must use different values for η to obtain the universal behavior for different charge carriers and surface orientations (electrons: 1/2 for (100) and 1/3 for (110), holes: 1/3).

These standard parameters provide mostly good universal behavior for a (100) surface orientation and low to moderate doping. For a (110) surface orientation, high-doping, or nonplanar and double-gate devices, the universal behavior is mostly not fully achieved. In

general, it remains a question of whether the use of this extraction method, and especially the use of the same η in the extraction from measurement and simulation, is correct.

If $\eta = 1$, E_{eff} corresponds exactly to the electric field at the interface in the depletion approximation. However, $\eta < 1$ lowers the field strength, thereby taking into account that the current flow is not only at the surface but also distributed a few nanometers into the depth of the silicon. Because it is not clear whether the field and current density distribution as well as the local dependency of the mobility on the electric field are described sufficiently in simulation, it may often be very difficult to achieve universal behavior in simulations with the same η parameter as in measurement.

In many cases, this universality is achieved only by introducing an artificial doping dependency for the SPS and SRS in the Lombardi terms for the mobility models. However, it is not clear whether this doping dependency exists at all, or whether it is only a result of this forced parameter fitting. It can result in an unusual situation where the mobility degradation in intrinsic or very low–doped regions is actually stronger than in high-doped regions and drops to completely unrealistic values.

Because of this, another extraction methodology is used for the mobility parameters. The mobility model is calibrated to the measured $\mu = \mu(N_{inv})$ curves. For this, no calibration of η is necessary, and universal behavior is not requested. After this, a check is performed with $\mu = \mu(E_{eff})$ but additional calibration is performed only when there are strong disagreements. Figure 7 to Figure 15 show the agreement between measurement and simulation.

In simulating CMOS devices with precalibrated parameter sets, you must always take into account that the precalibrated parameter sets are *initial* parameter sets that can undergo additional fine-tuning and major changes. The reasons are mainly connected with the dependency of the mobility degradation on the processing.

For example, the interface or surface roughness depends on the process conditions and the materials involved. Applying the parameters extracted above to modern FinFET devices with <110> channel direction, you can see that the inversion mobility is underestimated, which is connected to the fact that the surface roughness–related mobility degradation is smaller on the (110) fin sidewalls than in the planar (110) case [5].

Similarly, for the surface phonon–related interface mobility, the process conditions and the materials involved introduce some uncertainties that do not allow you to derive a parameter set that is valid for several device types or technology generations. Recalibration is mostly necessary.

The strength of RCS or RDS depends on the number of charges in the high-k gate stack and their position. The model must be calibrated to measurements when switching it on. RCS and RDS have the same origin: the mobility degradation by charges in the high-k gate stack. The difference is in the presence of both negative and positive charges in the case of RDS. For RPS, the parameters are extracted from MC simulation. Depending on the high-k gate stack

properties, fine-tuning may be necessary. However, because it is difficult to extract the correct parameters without having mobility measurements for different interfacial layer thicknesses and different temperatures, it is recommended to keep the parameters and to focus on the calibration of RCS and RDS.

The Philips unified mobility model (`PhuMob`) is calibrated to bulk mobility measurements. Usually, fine-tuning is necessary only when performing custom calibration with high-accuracy requirements. In addition, the mobility fine-tuning cannot be separated from the doping concentration or dopant activation calibration. Therefore, it is recommended that you keep the default parameters. When going to inversion layer conditions, 3D Coulomb scattering turns to 2D Coulomb scattering, the `PhuMob` model is switched off, and the 2D Coulomb scattering model takes over. The 2D Coulomb scattering model is a very simple description of reality with many fitting parameters. The influence of this model is mainly in the onset of the I–V curves. The default parameters are not very good. Additional calibration is necessary.

The stress dependency of the `hSubband` model for holes, the `eSubband` model for electrons, and the PMI model `MCmob` has been compared to the literature and in-house MC simulation.

For uniaxial stress dependencies, all three models show reasonable agreement. They are validated against MC simulation for selected non-uniaxial cases as well. However, fine-tuning of the stress influence on the mobility may be necessary during calibration: First, because the differences in the reference simulations in the literature [6][7][8] indicate that the modeling status is not good enough. Second, even when having the highest accuracy for the uniaxial stress curves, the calculation of arbitrary stress configurations must still be validated.

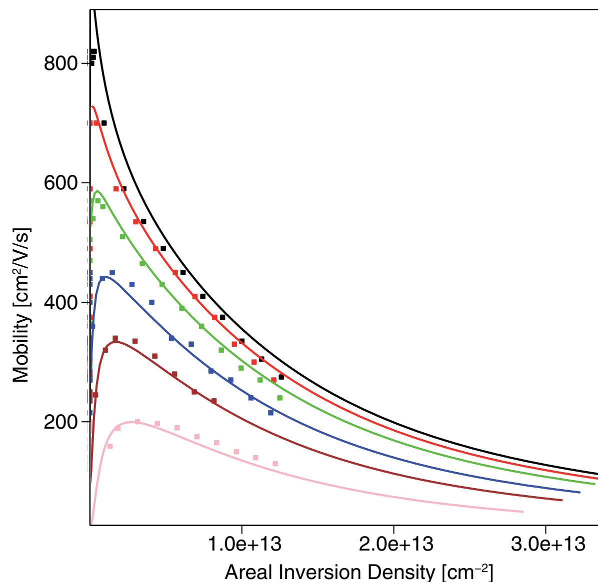

Figure 7 Electron mobility versus areal inversion density for (100) surface in linear scale (channel doping from top to bottom: 3.9e15, 2e16, 7.2e16, 3e17, 7.7e17, 2.4e18)

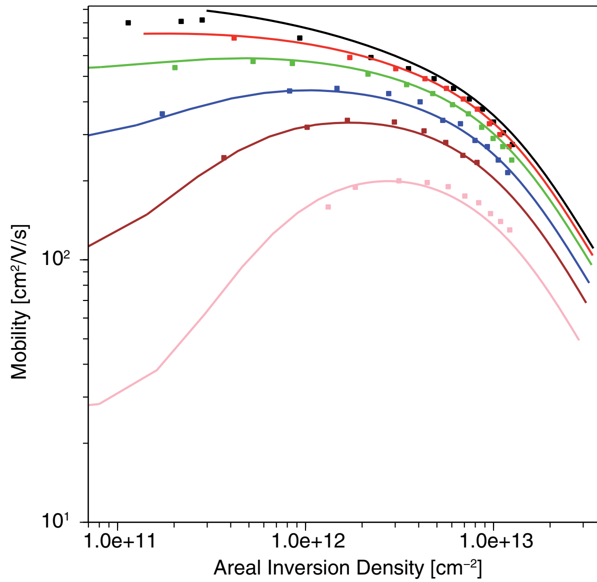

Figure 8 Electron mobility versus areal inversion density for (100) surface in logarithmic scale (channel doping from top to bottom: 3.9e15, 2e16, 7.2e16, 3e17, 7.7e17, 2.4e18)

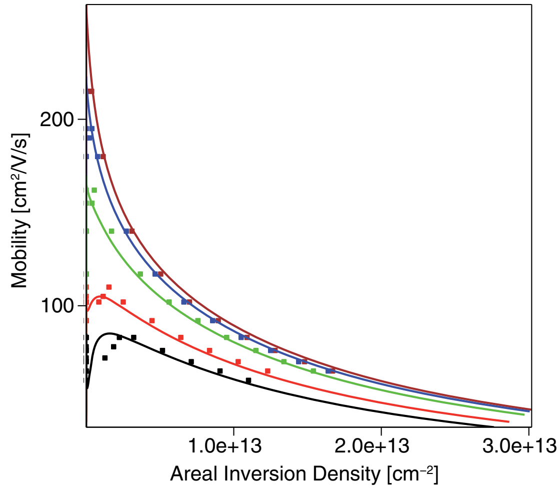

Figure 9 Hole mobility versus areal inversion density for (100) surface in linear scale (channel doping from top to bottom: 7.8e15, 1.6e16, 5.1e16, 2.7e17, 6.6e17)

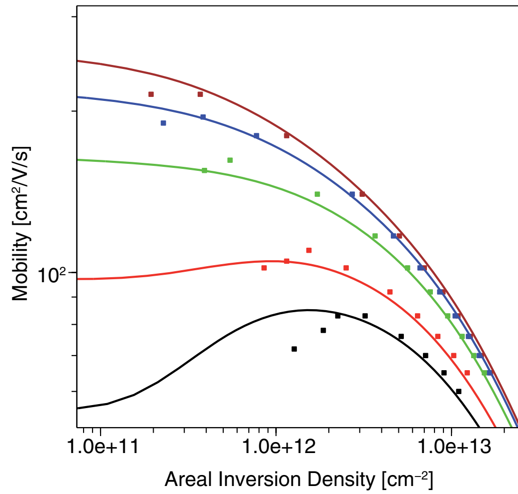

Figure 10 Hole mobility versus areal inversion density for (100) surface in logarithmic scale (channel doping from top to bottom: 7.8e15, 1.6e16, 5.1e16, 2.7e17, 6.6e17)

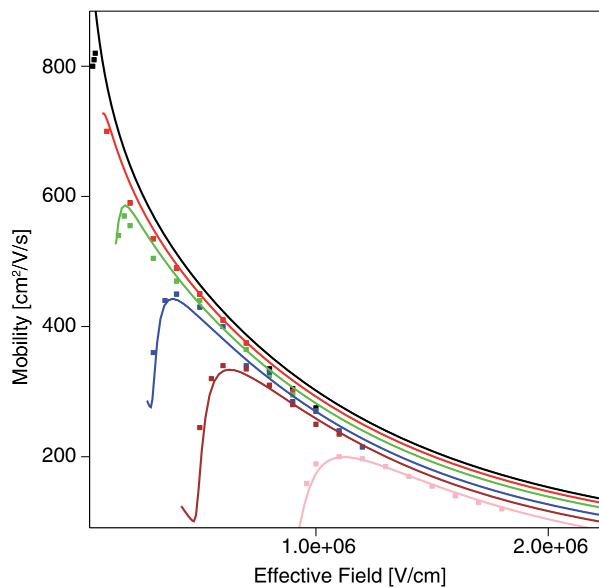

Figure 11 Electron mobility versus effective field for (100) surface in linear scale (channel doping from top to bottom: 3.9e15, 2e16, 7.2e16, 3e17, 7.7e17, 2.4e18)

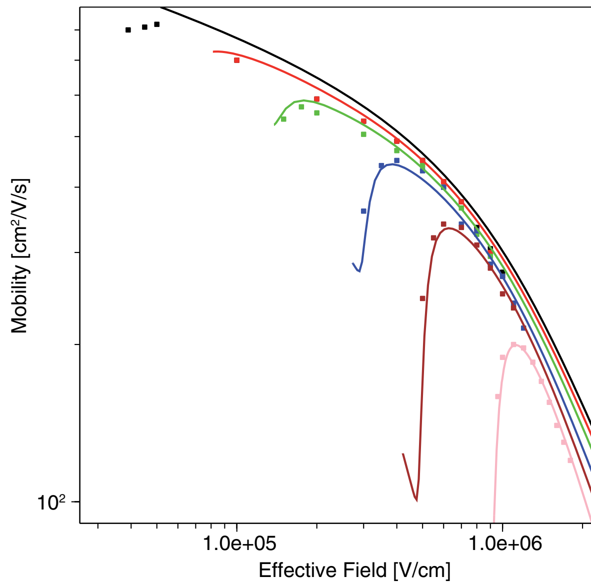

Figure 12 Electron mobility versus effective field for (100) surface in logarithmic scale (channel doping from top to bottom: 3.9e15, 2e16, 7.2e16, 3e17, 7.7e17, 2.4e18)

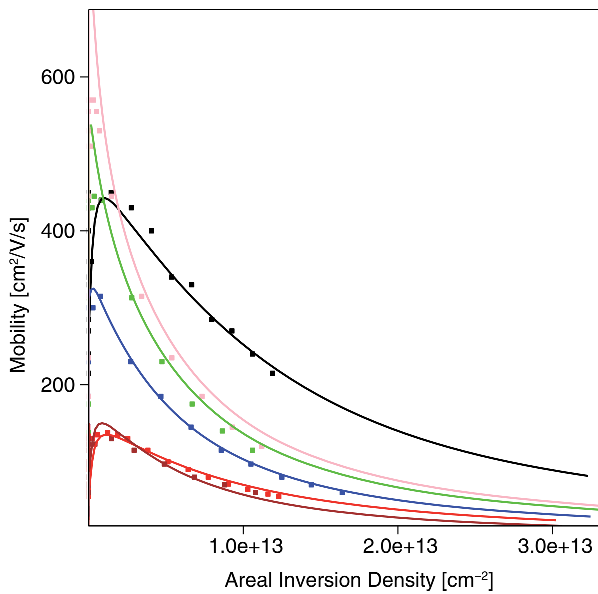

Figure 13 Electron mobility versus areal inversion density for (100) surface as a reference and for (110)/<100> and (110)/<110> in linear scale (channel doping between 5e17 and 9e17)

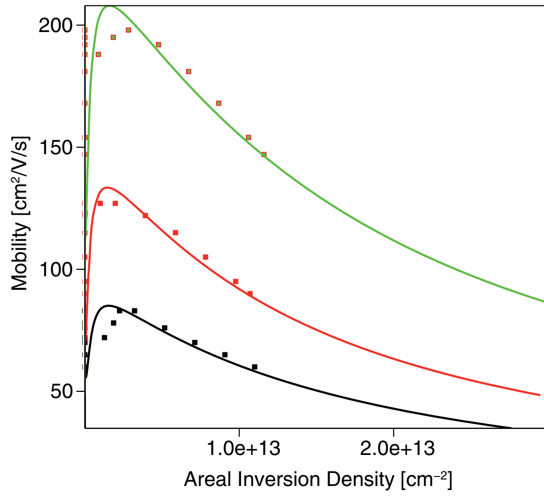

Figure 14 Hole mobility versus areal inversion density for (100) surface as a reference and for (110)/<100> and (110)/<110> in linear scale (channel doping between 4.5e17 and 6.6e17)

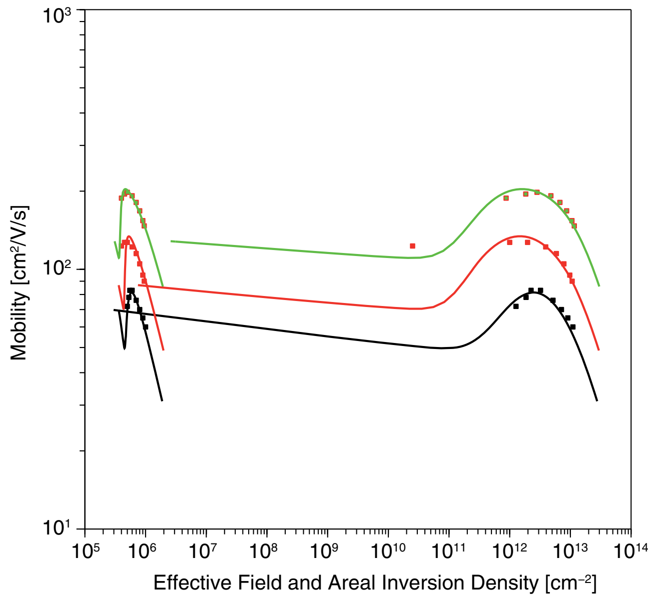

Figure 15 Hole mobility versus effective field and areal inversion density for (100) surface as a reference and for (110)/<100> and (110)/<110> in double logarithmic scale (channel doping between 4.5e17 and 6.6e17)

Basic Properties of Silicon Carbide Devices

The parameter values and the corresponding references also can be found in the parameter file `WBG.par` and in [9].

All SiC polytypes are indirect semiconductors, and the maximum of the upper valence bands is located at the center (Γ-point) of the Brillouin zone. Conduction band minima of 3C-SiC, 6H-SiC, and 4H-SiC are located at the points X, U on the (L-M) line, and M, respectively.

Photoluminescence or absorption measurements give an exciton band gap E_{gx}. There are no reliable measured values for binding energies E_x of free excitons, which are required to obtain the indirect band gap $E_g = E_{gx} + E_x$. As measured values of E_x range from 10–80 mV, a mean direct band gap may be assumed by shifting E_{gx} by 40 mV. In the parameter file, a value of `Eg0`=3.285 eV is finally used.

Temperature dependency of the band gap is measured for 6H-SiC in the temperature ranges from 6 K to 200 K, and from 300 K to 700 K. The dependency of 3C-SiC is measured in the temperature range from 295 K to 700 K. The respective dependency of 4H-SiC is assumed to be similar because no experimental data is available.

The effective mass of electrons and holes has been measured by optically detected cyclotron resonance, or Raman scattering, and has been compared to theoretical calculation. Theoretical calculation reproduced well the experimental results.

There is no publication on measured data of bandgap narrowing. The theoretical calculation was first done by Lindefelt [10] and followed by Persson *et al*. [11]. The former model constitutes an extension of a semiempirical method originally developed by Jain and Roulston [12]. The latter is based upon random phase approximation. Both calculations give the analytic form of band-edge displacement depending on the doping density. The analytic form corresponds to the `JainRoulston` model implemented in Sentaurus Device.

Figure 16 on page 49 compares results from [10] and [11] with the Slotboom model implemented in Sentaurus Device with calibrated coefficients.

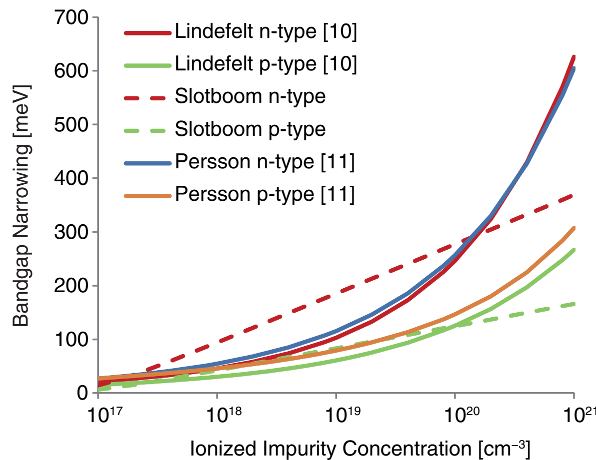

Figure 16 Bandgap narrowing of 4H-SiC [10][11]

Electron affinity is calculated assuming the linear dependency of hexagonality together with the measured band offset of the conduction band for 3C/6H and the calculated result of the band offset of the valence band.

Parameter sets for the Hatakeyama model and the Okuto– Crowell impact ionization model are implemented in the parameter files (see Chapter 6 on page 37).

Temperature dependency of thermal conductivity of 4H-SiC and 6H-SiC perpendicular to the c-axis has been reported in the literature. At low temperatures, T^3 dependency and T^2 dependency are observed for 4H-SiC and 6H-SiC, respectively. T^2 dependency is attributed to the scattering of phonons by electrons in the impurity band. Thermal conductivity in 6H-SiC single crystals decreases with increasing electron concentration, and the slope at low temperature can be represented by the T^2 law, which confirms the dominance of electron scattering. The temperature dependency of thermal conductivity using data of [13], [14], [15], and [16] as cited in [17] is implemented in the parameter files (see Chapter 6 on page 37). The experimental data is that in the direction perpendicular to the c-axis.

Parameter sets for the Masetti and the Arora doping-dependent mobility models are implemented in the parameter files (see Chapter 6 on page 37). Figure 17 and Figure 18 show a comparison with different literature data.

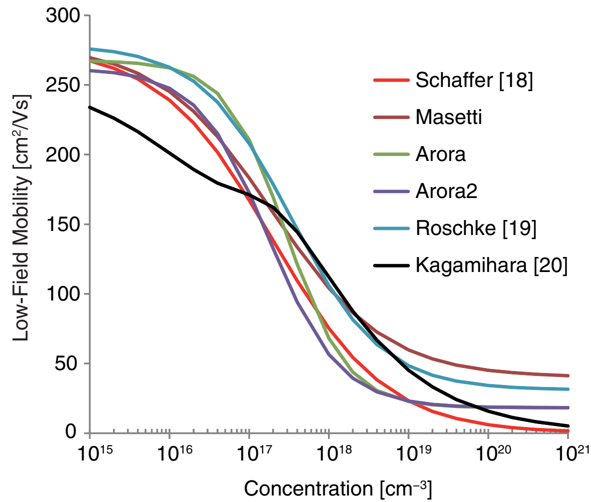

Figure 17   Doping-dependent electron mobility at 500 K for n-doped 4H-SiC [18][19][20]

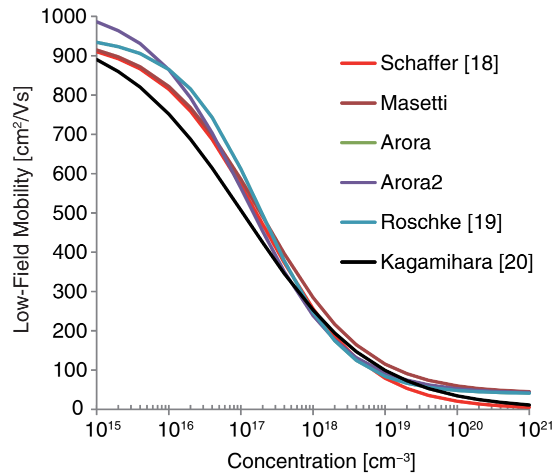

Figure 18   Doping-dependent electron mobility at 300 K for n-doped 4H-SiC [18][19][20]

For high-field saturation, all measured data refers to the current flow perpendicular to the c-axis. Parameters for the Canali model are extracted and implemented in the parameter file.

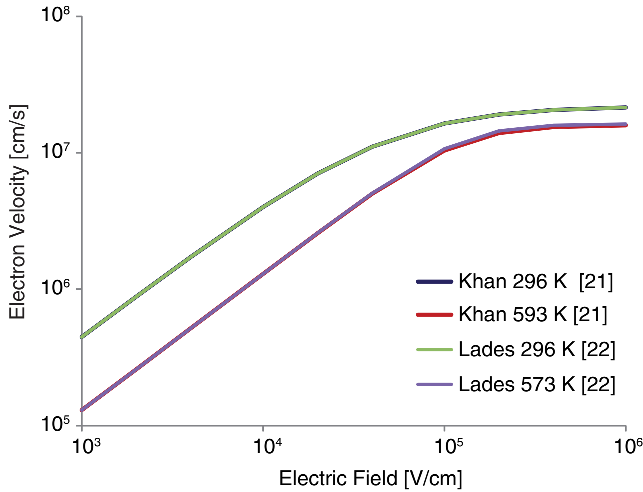

Figure 19 Drift velocity of electrons in 4H-SiC, parallel to basal plane (0001) [21][22]

A nitrogen atom residing on the C lattice site serves as the shallow donor in SiC. Phosphorus also is used as a shallow donor (like nitrogen) and has approximately the same ionization energy Ec-93 meV at the cubic site and Ec-53 meV at the hexagonal site. However, unlike nitrogen, P mainly substitutes at a silicon site, and less than 10% of substitutional P is at C sites. At C sites, P has a slightly larger ionization energy than that at the Si site. The ionization energy of N and P donors decreases with increasing donor concentration. Experimental data for cubic and hexagonal N donors in 6H-SiC is available. For N donors in 4H-SiC, experimental data of donor concentration dependency and fitting with empirically formula has been reported. Figure 20, Figure 21, Figure 22, and Figure 23 show the experimental data and the fit implemented in the parameter file.

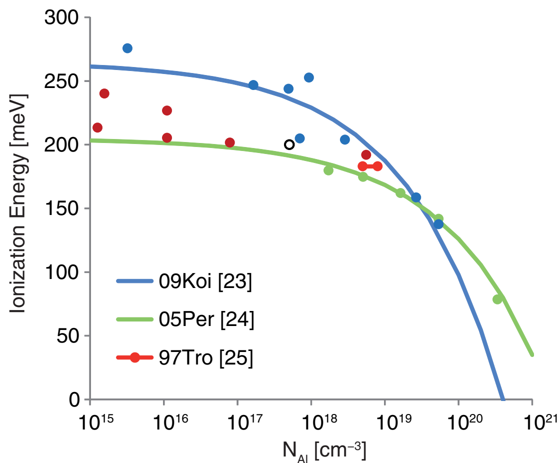

Figure 20 Ionization energy for aluminum-doped 4H-SiC together with extracted fit function [23][24][25]

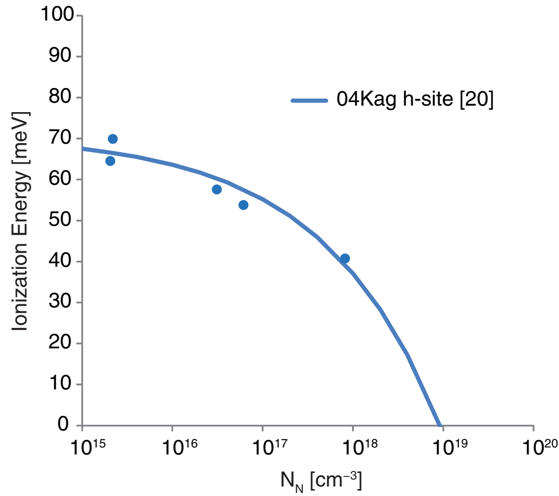

Figure 21 Ionization energy for nitrogen-doped 4H-SiC (hexagonal site) together with extracted fit function [20]

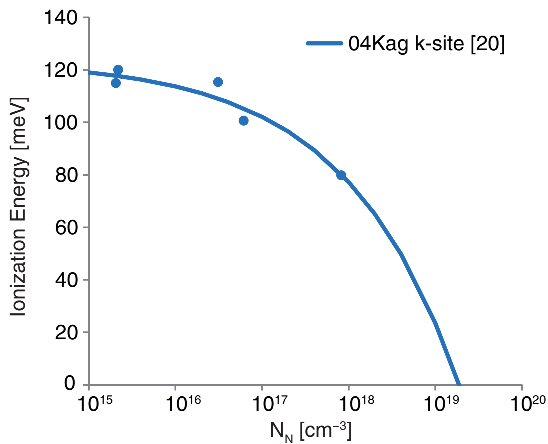

Figure 22 Ionization energy for nitrogen-doped 4H-SiC (cubic site) together with extracted fit function [20]

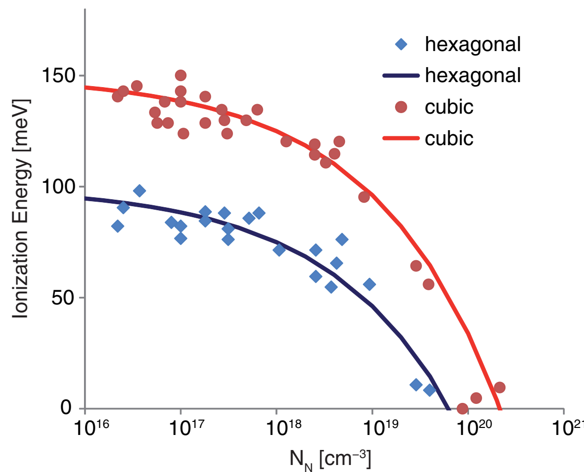

Figure 23 Ionization energy for nitrogen-doped 6H-SiC together with extracted fit function

References

[1] S. Takagi *et al.*, "On the Universality of Inversion Layer Mobility in Si MOSFET's: Part I—Effects of Substrate Impurity Concentration," *IEEE Transactions on Electron Devices*, vol. 41, no. 12, pp. 2357–2362, 1994.

[2] S. Takagi *et al.*, "On the Universality of Inversion Layer Mobility in Si MOSFET's: Part II—Effects of Surface Orientation," *IEEE Transactions on Electron Devices*, vol. 41, no. 12, pp. 2363–2368, 1994.

[3] H. Nakamura *et al.*, "Effects of Selecting Channel Direction in Improving Performance of Sub-100 nm MOSFETs Fabricated on (110) Surface Si Substrate," *Japanese Journal of Applied Physics*, vol. 43, no. 4B, pp. 1723–1728, 2004.

[4] H. M. Nayfeh *et al.*, "Influence of High Channel Doping on the Inversion Layer Electron Mobility in Strained Silicon n-MOSFETs," *IEEE Electron Device Letters*, vol. 24, no. 4, pp. 248–250, 2003.

[5] C. D. Young *et al.*, "(110) and (100) Sidewall-oriented FinFETs: A performance and reliability investigation," *Solid-State Electronics*, vol. 78, pp. 2–10, December 2012.

[6] A. T. Pham, C. Jungemann, and B. Meinerzhagen, "Modeling and validation of piezoresistive coefficients in Si hole inversion layers," *Solid-State Electronics*, vol. 53, no. 12, pp. 1325–1333, 2009.

[7] F. M. Bufler, A. Erlebach, and M. Oulmane, "Hole Mobility Model With Silicon Inversion Layer Symmetry and Stress-Dependent Piezoconductance Coefficients," *IEEE Electron Device Letters*, vol. 30, no. 9, pp. 996–998, 2009.

[8] P. Packan *et al.*, "High Performance Hi-K + Metal Gate Strain Enhanced Transistors on (110) Silicon," in *IEDM Technical Digest*, San Francisco, CA, USA, December 2008.

[9] Y. Asahi, *Physical parameters for 4H-SiC and 6H-SiC*, Internal Report, Mountain View, California: Synopsys, Inc., November 2012.

[10] U. Lindefelt, "Doping-induced band edge displacements and band gap narrowing in 3C–, 4H–, 6H–SiC, and Si," *Journal of Applied Physics*, vol. 84, no. 5, pp. 2628–2637, 1998.

[11] C. Persson, U. Lindefelt, and B. E. Sernelius, "Bang gap narrowing in n-type and p-type 3C–, 2H–, 4H–, 6H–SiC, and Si," *Journal of Applied Physics*, vol. 86, no. 8, pp. 4419–4427, 1999.

[12] S. C. Jain and D. J. Roulston, "A Simple Expression for Band Gap Narrowing (BGN) in Heavily Doped Si, Ge, GaAs and Ge_xSi_{1-x} Strained Layers," *Solid-State Electronics*, vol. 34, no. 5, pp. 453–465, 1991.

[13] Y. S. Touloukian and E. H. Buyco, *Specific Heat–Nonmetallic Solids*, Thermophysical Properties of Matter, TPRC Data Series, vol. 5, IFI/Plenum: New York, 1970.

[14] Y. S. Touloukian and C. Y. Ho (eds.), *Thermal Conductivity–Nonmetallic Solids*, Thermophysical Properties of Matter, TPRC Data Series, vol. 2, IFI/Plenum: New York, 1970.

[15] E. A. Burgemeister, W. von Muench, and E. Pettenpaul, "Thermal conductivity and electrical properties of 6*H* silicon carbide," *Journal of Applied Physics*, vol. 50, no. 9, pp. 5790–5794, 1979.

[16] D. Morelli *et al.*, "Carrier concentration dependence of the thermal conductivity of silicon carbide," in *5th Silicon Carbide and Related Materials Conference*, Washington, DC, USA, pp. 313–315, November 1993.

[17] D. T. Morelli *et al.*, "Phonon-electron scattering in single crystal silicon carbide," *Applied Physics Letters*, vol. 63, no. 23, pp. 3143–3145, 1993.

[18] W. J. Schaffer *et al.*, "Conductivity Anisotropy in Epitaxial 6H and 4H SiC," in *MRS Symposium Proceedings, Diamond, SiC and Nitride Wide Bandgap Semiconductors*, vol. 339, San Francisco, CA, USA, pp. 595–600, April 1994.

[19] M. Roschke and F. Schwierz, "Electron Mobility Models for 4H, 6H, and 3C SiC," *IEEE Transactions on Electron Devices*, vol. 48, no. 7, pp. 1442–1447, 2001.

[20] S. Kagamihara *et al.*, "Parameters required to simulate electric characteristics of SiC devices for *n*-type 4H–SiC," *Journal of Applied Physics*, vol. 96, no. 10, pp. 5601–5606, 2004.

[21] I. A. Khan and J. A. Cooper, Jr., "Measurement of High Field Electron Transport in Silicon Carbide," *Materials Science Forum*, vol. 264-268, pp. 509–512, February 1998.

[22] M. Lades, *Modeling and Simulation of Wide Bandgap Semiconductor Devices: 4H/6H-SiC*, Ph.D. thesis, Technischen Universität, Munich, Germany, 2000.

[23] A. Koizumi, J. Suda, and T. Kimoto, “Temperature and doping dependencies of electrical properties in Al-doped 4*H*-SiC epitaxial layers,” *Journal of Applied Physics*, vol. 106, no. 1, p. 013716, 2009.

[24] J. Pernot, S. Contreras and J. Camassel, “Electrical transport properties of aluminum-implanted 4H–SiC,” *Journal of Applied Physics*, vol. 98, no. 2, p. 023706, 2005.

[25] T. Troffer *et al.*, “Doping of SiC by Implantation of Boron and Aluminum,” *Physica Status Solidi (a)*, vol. 162, no. 1, pp. 277–298, 1997.

APPENDIX A Description of PMI Model MCmob

This appendix describes the PMI model MCmob and its parameters.

Overview

The physical model interface (PMI) model `MCmob` of Sentaurus Device is based on nonlinear relations between the mobility enhancement and the stress components where the coefficients of the equations are extracted from Monte Carlo simulation, from Sentaurus Band Structure simulation, or from other reference data or tools. The command file section for `MCmob` is explained in Chapter 3 on page 5.

The features of the PMI model are:

- Calculation of the hole mobility enhancement by stress for silicon and SiGe for mole fractions from 0% to 100% for the channel direction and wafer orientation combinations <110>/(001) and <110>/(1$\underline{1}$0).
- Calculation of the hole and electron mobility enhancement by stress for silicon for the channel direction and wafer orientation combinations <100>/(001), <110>/(001), and <110>/(1$\underline{1}$0).
- Parameter interface that allows complete user-defined parameter sets.
- Crystallographic surface or interface orientation is determined automatically.

The PMI model is designed for semiconductor–isolator interfaces as in an MIS structure where the bulk symmetry typical for the standard piezo model is broken. This makes it necessary to determine the direction of the interface normal with respect to the device coordinate system. Currently, this detection is not performed fully and automatically, and the specification of parameters in the Sentaurus Device parameter file is necessary (see Parameters on page 58).

The default dataset is generated from Sentaurus Device Monte Carlo simulation.

Parameters

The PMI model allows the following parameter settings:

`autoorientation`

Switches detection of crystallographic surface orientation:
`0`: No detection of crystallographic surface orientation but crystallographic surface orientation is defined by `waferori`.
`1`: Detection of crystallographic surface orientation.
`2`: Detection of crystallographic surface orientation and adaptation of local coordinate system (coordinate system used for matching the stress components to MIS plane orientation and channel direction at each mesh node) for FinFET-like structures with <110> channel orientation.
`3`: Detection of crystallographic surface orientation; local coordinate systems are detected and defined using parameters in the Sentaurus Device parameter file.

`channelori`

Sets the channel direction:
`0`: <110>
`1`: <100>

`waferori`

Sets the wafer orientation; used when `autoorientation=0`:
`0`: (001)
`1`: $(1\bar{1}0)$

`coordinatesystem`

Global coordinate system in Sentaurus Device (default: `0`).

`ConstantMoleFraction`

Switches between reading the mole-fraction distribution from a TDR file and setting the constant mole fraction in the parameter file:
`0`: Read from TDR file.
`1`: User sets mole fraction in Sentaurus Device parameter file.

`ConstantStress`

Switches between reading the distribution of stress components from a TDR file and setting the constant stress components in the parameter file:
`0`: Read from TDR file.
`1`: User sets constant stress components in Sentaurus Device parameter file.

`DeltaMuPrefactorx`

Scales the mobility enhancement caused by stress in the current flow direction.

`DeltaMuPrefactory`

Scales the mobility enhancement caused by stress normal to the MIS interface.

`DeltaMuPrefactorz`	Scales the mobility enhancement caused by stress in-plane with the MIS interface and normal to the current direction.
`referenceplanecoordinatex1`	Coordinate of first reference plane in the x-direction of the device coordinate system (yz plane, default: 1e6).
`referenceplanecoordinatex2`	Coordinate of second reference plane in the x-direction of the device coordinate system (yz plane, default: 1e6).
`referenceplanecoordinatey1`	Coordinate of first reference plane in the y-direction of the device coordinate system (xz plane, default: 1e6).
`referenceplanecoordinatey2`	Coordinate of second reference plane in the y-direction of the device coordinate system (xz plane, default: 1e6).
`referenceplanecoordinatez1`	Coordinate of first reference plane in the z-direction of the device coordinate system (xy plane, default: 1e6).
`referenceplanecoordinatez2`	Coordinate of second reference plane in the z-direction of the device coordinate system (xy plane, default: 1e6).
`referenceplanesystemx1`	Defines the local coordinate system for the reference plane parallel to the yz plane at the position `x=referenceplanecoordinatex1` (default: –1).
`referenceplanesystemx2`	Defines the local coordinate system for the reference plane parallel to the yz plane at the position `x=referenceplanecoordinatex2` (default: –1).
`referenceplanesystemy1`	Defines the local coordinate system for the reference plane parallel to the xz plane at the position `y=referenceplanecoordinatey1` (default: –1).
`referenceplanesystemy2`	Defines the local coordinate system for the reference plane parallel to the xz plane at the position `y=referenceplanecoordinatey2` (default: –1).
`referenceplanesystemz1`	Defines the local coordinate system for the reference plane parallel to the xy plane at the position `y=referenceplanecoordinatez1` (default: –1).
`referenceplanesystemz2`	Defines the local coordinate system for the reference plane parallel to the xy plane at the position `y=referenceplanecoordinatez2` (default: –1).
`Stress_xx`	S_{xx} stress component in the device coordinate system when `ConstantStress=1`.

`Stress_yy`	S_{yy} stress component in the device coordinate system when `ConstantStress=1`.
`Stress_zz`	S_{zz} stress component in the device coordinate system when `ConstantStress=1`.
`MoleFraction`	SiGe mole fraction when `ConstantMoleFraction=1`.

For planar devices with one conducting MIS plane, the default parameters can be kept and no additional information is necessary when a device coordinate system has the configuration: x – channel direction, y – normal to the MIS interface, z – in-plane with the MIS interface but normal to the channel direction and the wafer orientation equals (100).

For other device coordinate systems and one conducting MIS plane, the parameter `coordinatesystem` must be specified in the Sentaurus Device parameter file:

- Device coordinate system:
  x: Channel direction
  z: Direction normal to the MIS interface
  y: In-plane with the MIS interface but normal to the channel direction (`coordinatesystem=1`)
- Device coordinate system:
  y: Channel direction
  x: Direction normal to the MIS interface
  z: In-plane with the MIS interface but normal to the channel direction (`coordinatesystem=2`)
- Device coordinate system:
  y: Channel direction
  z: Direction normal to the MIS interface
  x: In-plane with the MIS interface but normal to the channel direction (`coordinatesystem=3`)
- Device coordinate system:
  z: Channel direction
  x: Direction normal to the MIS interface
  y: In-plane with the MIS interface but normal to the channel direction (`coordinatesystem=4`)
- Device coordinate system:
  z: Channel direction
  y: Direction normal to the MIS interface
  x: In-plane with the MIS interface but normal to the channel direction (`coordinatesystem=5`)

For nonplanar devices with more than one conducting MIS plane, for example FinFETs, `autoorientation=2` provides automatic detection of the surface orientation and the

coordinate system for FinFETs with <110> channel direction. For general applications and for FinFETs with channel direction <100> and wafer orientation (100), the local coordinate system must be defined manually in the Sentaurus Device parameter file by using the reference plane system parameters:

- Local coordinate system for a MIS interface in the xz plane close to `referenceplanecoordinatey1` or `referenceplanecoordinatey2`:
  x: Channel direction
  y: Direction normal to the MIS interface
  z: In-plane with the MIS interface but normal to the channel direction (`referenceplanesystemy1=0` or `referenceplanesystemy2=0`)
- Local coordinate system for a MIS interface in the xz plane close to `referenceplanecoordinatey1` or `referenceplanecoordinatey2`:
  z: Channel direction
  y: Direction normal to the MIS interface
  x: In-plane with the MIS interface but normal to the channel direction (`referenceplanesystemy1=1` or `referenceplanesystemy2=1`)
- Local coordinate system for a MIS interface in the xy plane close to `referenceplanecoordinatez1` or `referenceplanecoordinatez2`:
  x: Channel direction
  z: Direction normal to the MIS interface
  y: In-plane with the MIS interface but normal to the channel direction (`referenceplanesystemz1=0` or `referenceplanesystemz2=0`)
- Local coordinate system for a MIS interface in the xy plane close to `referenceplanecoordinatez1` or `referenceplanecoordinatez2`:
  y: Channel direction
  z: Direction normal to the MIS interface
  x: In-plane with the MIS interface but normal to the channel direction (`referenceplanesystemz1=1` or `referenceplanesystemz2=1`)
- Local coordinate system for a MIS interface in the yz plane close to `referenceplanecoordinatex1` or `referenceplanecoordinatex2`:
  y: Channel direction
  x: Direction normal to the MIS interface
  z: In-plane with the MIS interface but normal to the channel direction (`referenceplanesystemx1=0` or `referenceplanesystemx2=0`)
- Local coordinate system for a MIS interface in the yz plane close to `referenceplanecoordinatex1` or `referenceplanecoordinatex2`:
  z: Channel direction
  x: Direction normal to the MIS interface
  y: In-plane with the MIS interface but normal to the channel direction (`referenceplanesystemx1=1` or `referenceplanesystemx2=1`)

For the simulation of a planar MIS transistor, the use of the parameters `waferori` and `coordinatesystem` is sufficient. Instead of using `waferori`, `autoorientation=1` can be

used to detect automatically the crystallographic wafer or surface orientation. In this case, `waferori` is overwritten by the automatically detected orientation. For FinFET devices with <110> channel direction, `autoorientation=2` can be used to allow automatic detection of the surface orientation and the local coordinate system. For other applications or for FinFETs with channel orientation <100>, the reference plan parameters can be used to define the local coordinate system where the crystallographic surface orientation is detected automatically. For that, `autoorientation=3` must be used.

The following examples illustrate the use of the parameters for orientation and coordinate system.

Example 1

Planar MISFET with wafer orientation (100) and device coordinate system x-channel direction, y-wafer normal direction, z-device width direction:

Default parameters can be used.

Example 2

Planar MISFET with wafer orientation (100) and device coordinate system x-channel direction, z-wafer normal direction, y-device width direction:

```
coordinatesystem=1
```

Example 3

Planar MISFET with wafer orientation (110) and device coordinate system with x-channel direction, z-wafer normal direction, y-device width direction:

```
coordinatesystem=1
autoorientation=1
```

or:

```
coordinatesystem=1
waferori=1
```

Example 4

FinFET with wafer orientation (100), channel orientation <110>, and device coordinate system with x-channel direction, y-wafer normal direction, z-device width direction:

```
autoorientation=2
```

Example 5

FinFET with wafer orientation (100), channel orientation <110>, and device coordinate system with x-channel direction, z-wafer normal direction, y-device width direction:

```
coordinatesystem=1
autoorientation=2
```

Example 6

FinFET with wafer orientation (100), channel orientation <100>, and device coordinate system with x-channel direction, z-wafer normal direction, y-device width direction:

```
coordinatesystem=1
autoorientation=3
referenceplanesystemy1=0
referenceplanesystemy2=0
referenceplanesystemz1=0
referenceplanecoordinatey1=-@W/2.0@
referenceplanecoordinatey2=@W/2.0@
referenceplanecoordinatez1=@H@
```

Figure 24 shows a FinFET device with geometry.

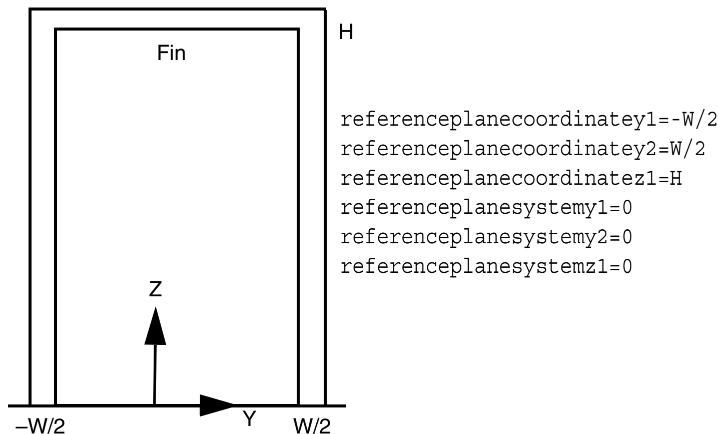

Figure 24 Cross section of FinFET structure normal to the channel direction with height (H) and width (W); the origin of the coordinate system is at y=0 and z=0

The PMI has a parameter interface that allows you to change all coefficients of the fit and interpolation functions. In this way, you can define the mobility response to mechanical stress using the Sentaurus Device parameter file.

Corresponding parameter files and explanations are available upon request. Contact TCAD Support (see Contacting Your Local TCAD Support Team Directly on page viii) or Consulting and Engineering (tcad-services@synopsys.com).